ТВЕРДОТЕЛЬНАЯ ЭЛЕКТРОНИКА, МИКРО- И НАНОЭЛЕКТРОНИКА

ПРИБОРЫ МАГНОННОЙ ЛОГИКИ

А. Г. Хитун, А. Е. Кожанов

Хитун Александр Георгиевич, кандидат физико-математических наук, профессор факультета электроники и компьютерной техники, Университет Калифорнии, Риверсайд, akhitun@ece.ucr.edu

Кожанов Александр Евгеньевич, кандидат физико-математических наук, доцент факультета физики и астрономии, Университет штата Джорджия, Атланта, akozhanov@gsu.edu

Делается обзор работ по исследованиям и разработкам физико-технологической платформы создания устройств магнонной логики. Рассматриваются физические принципы построения устройств спиновой логики, методы управления фазой и эффекты интерференции спиновых волн при распространении в магнитных микроструктурах. Обсуждаются результаты микромагнитного моделирования и экспериментальных исследований эффектов распространения спиновых волн в микроволноводах на основе ферромагнитных металлов и пленок ферритов гранатов. Рассматриваются методы возбуждения и приема спиновых волн в магнитных волноведущих структурах. Определенное внимание уделяется архитектуре и подходам к построению логических устройств на основе интерференционных эффектов. Для мультиферроидных структур приводятся оценки энергоэффективности переключения устройств магнонной логики между состояниями логический «0» и «1». Показана возможность построения основных логических элементов и функций на принципах магнонной логики. Проводится сравнение магнонных логических устройств с устройствами по стандартной КМОП-технологии. Обсуждаются возможные области применения устройств магнонной логики.

Ключевые слова: магноника, спиновые волны, тонкие магнитные пленки, мультиферроики, стрейнтроника, магнонные сети и волноведущие структуры, интерференция спиновых волн, управление фазой спиновых волн, магнонная голографическая память.

## MAGNONIC LOGIC DEVICES

A. G. Khitun, A. E. Kozhanov

Alexander G. Khitun, ORCID 0000-0003-4501-4687, University of California – Riverside, 900, University Ave., Engineering Bldg. II, Suite 414, Riverside, CA 92521, United States, akhitun@ece.ucr.edu

Alexander E. Kozhanov, ORCID 0000-0003-1324-1332, Georgia State University, Office: 408 Science Annex Bldg., 25 Park pl NE, rm 605, Atlanta, GA 30303, United States, akozhanov@gsu.edu

Background and Objectives: There is a big impetus for the development of novel computational devices able to overcome the limits of the traditional transistor-based circuits. The utilization of phase in addition to amplitude is one of the promising approaches towards more functional computing architectures. In this work, we present an overview on magnonic logic devices utilizing spin waves for information transfer and processing. **Materials and Methods:** Magnonic logic devices combine input/output elements for spin wave generation/detection and
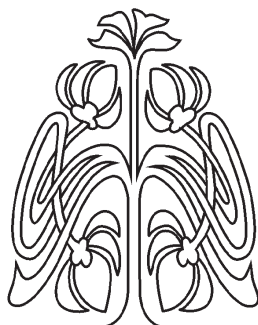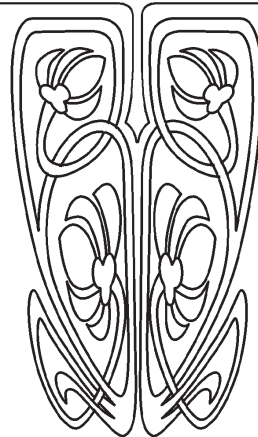
an analog core. The core consists of magnetic waveguides serving as a spin wave buses. The data transmission and processing within the analog part is accomplished by the spin waves, where logic 0 and 1 are encoded into the phase of the propagating wave. The latter makes it possible to utilize spin wave interference for logic functionality. The proof-of-concept experiments were accomplished on micrometer scale ferromagnetic $Ni_{81}Fe_{19}$ and ferrite $Y_3Fe_2(FeO_4)_3$ structures. **Results:** We present experimental data on spin wave propagation and interference in magnetic microstructures. We also present experimental data showing parallel read-out of magnetic bits using spin wave interference. Based on the obtained results, we consider possible logic circuits and architectures. **Conclusion:** Magnonic logic devices may offer a significant functional throughput enhancement over the conventional logic circuits by exploiting phase in addition to amplitude. It is also possible to construct non-volatile magnonic logic circuits with built-in magnetic memory. Magnonic logic devices such as magnonic holographic memory are aimed not to replace but to complement the existing logic circuitry in special task data processing.

Key words: Magnonic Logic Devices, multilevel logic, spin waves.

1. Introduction on spin waves

The rapid approach to the scaling limit of metal-oxide semiconductor field-effect transistor (MOSFET) has stimulated a great deal of interest to research alternative technologies, which may overcome the constrains inherent to complementary metal-oxide-semiconductor (CMOS) -based circuitry and thus provide a route to more functional and less power consuming logic devices. As one of possible directions, Spintronics has been recognized as a new emerging approach [1] aimed to take the advantage of using spin in addition or instead of an electric charge. Spin wave-based logic devices constitute one of the possible approaches offering an alternative mechanism for information transfer and processing. Spin wave is a collective precession of spins in a spin lattice around the direction of magnetization. Similar to the lattice waves (phonons) in solid systems, spin wave appear in magnetically ordered structures, and a quantum of spin wave is called a "magnon". Spin waves has attracted scientific interest for a long time [2]. Spin wave propagation has been studied in a variety of magnetic materials and nanostructures [3–6]. Relatively slow group velocity (more than two orders of magnitude slower than the speed of light) and high attenuation (more than six orders of magnitude higher attenuation than for photons in a standard optical fiber) are two well-known disadvantages, which explain the lack of interest in spin waves as a potential candidate for information transmission. The situation has changed drastically as the characteristic distance between the devices on the chip entered the deep-submicron range. It has become more important to have fast signal conver-

sion/modulation, while the short traveling distance compensates slow propagation and high attenuation. From this point of view, spin waves possess certain technological advantages: (i) spin waves can be guided in the magnetic waveguides similar to the optical fibers; (ii) spin wave signal can be converted into a voltage via inductive coupling, spin torque or multiferroic elements; (iii) magnetic field can be used as an external parameter for sin wave signal modulation. The wavelength of the exchange spin waves can be as short as several nanometers, and the coherence length may exceed tens of microns at room temperature. The latter translates in the intriguing possibility of building scalable logic devices utilizing spin wave inherent properties. Starting the first publication on the spin wave logic circuits [7], there have been a number of works on the spin wave logic devices and circuits [7–13]. In this Chapter we present recent developments on spin wave- (magnonic) logic circuits and discuss their potential advantages and shortcoming. We start our consideration with the description of the basic elements requiring for logic circuits construction including spin wave generation, detection, waveguides, waveguide junctions, and phase shifters [14]. There are several physical mechanisms for spin wave generation and detection by using micro-antennas [3, 4], spin torque and spin hall oscillators [15], and multiferroic elements [16]. These elements are aimed to convert the input electric signals into spin waves, and vice versa, convert the output spin waves into the electric signals. Basic principle of spin wave excitation utilizes a local application of torque to the magnetic moments by local magnetic field (dipolar or exchange) or spin polarized electrons. For example, micro-antenna is a conducting contour placed in the vicinity of the spin wave bus. An electric current passed through the contour generates a magnetic field around the current-carrying wires, which excites spin waves in the magnetic material. The polarity of the input pulse defines the direction of the current through the loop (clockwise or counter clockwise), and, thus, defines the initial phase (0 or π) of the excited spin wave signal. A propagating spin wave induces a disturbance of local magnetization and changes the magnetic flux. According to Faraday's law, the change of the magnetic flux induces an inductive voltage in a conductor loop, which magnitude is proportional to the rate of the magnetic flux change. The same conductor loop can be used for the detection of the inductive voltage produced by the spin wave. Coplanar microstrip coupling loops are widely used for spin wave excitation/detection and the detailed

description of the experimental technique can be found everywhere [3–5]. Poor coupling between microwave signal and spin waves is one of the main disadvantages of this approach. Due to the high magnetic susceptibility of the magnetic media the microwave magnetic field generated by the antennas stays primarily outside of the spin waveguides thus reducing efficiency of the spin wave excitation. It was shown that lithographically "wrapping" the magnetic material around the microstrip as shown in the Figure 1 results in microwave magnetic field confinement within the spin waveguide thus significantly enhancing the spin wave excitation/detection

efficiency [13, 17]. Length of ferromagnetic tubes thus formed defines the range of the accessible spin wave wavelengths. Although the microstrip antennas are the most common technique used to study spin waves in structured ferromagnetic films, spin wave detection using this technique allows only a limited scaling. Decrease of a spin wave device size is followed by the amount of magnetic moments that induce currents in the detecting microstrip antennas. Spin wave detection in structures with spin waveguide thicknesses less than approximately 20nm becomes challenging. At the nano-scale other spin wave excitation techniques can be used.
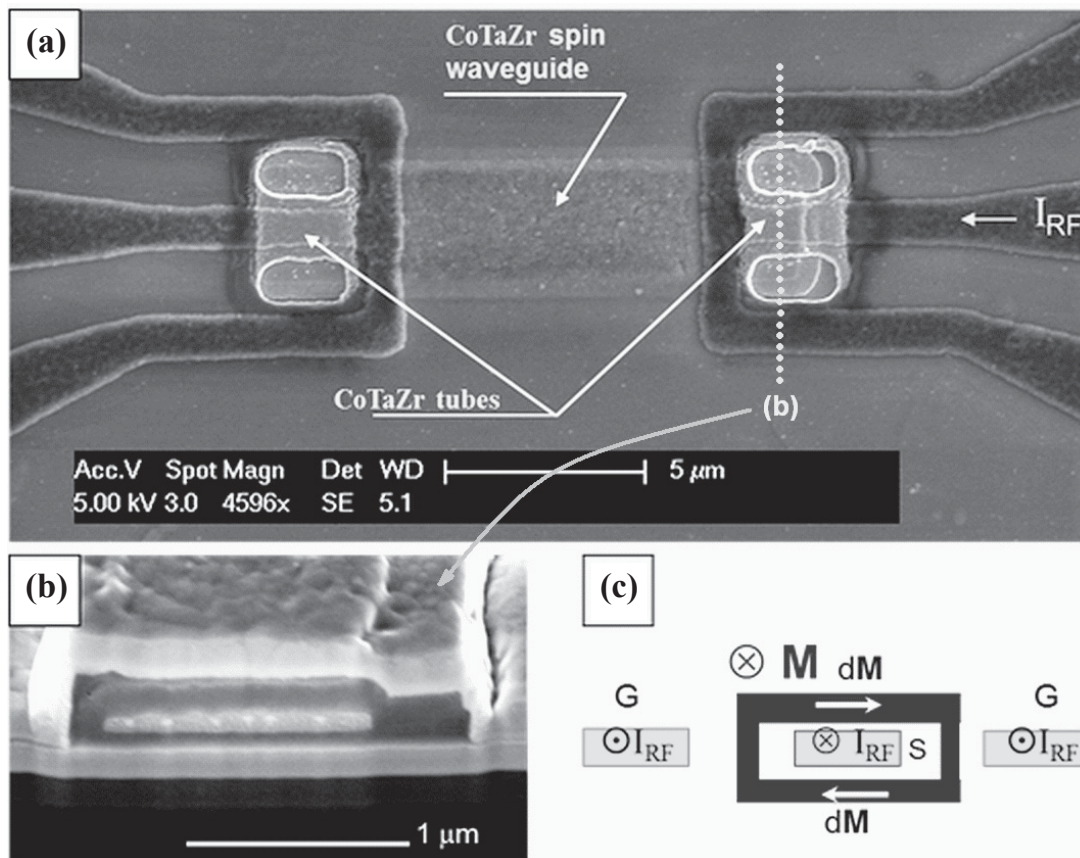

Fig. 1. Top view SEM micrograph of ferromagnetic CoTaZr spin waveguide with ferromagnetic tube couplers at its ends (a). Tube coupler cross sectional SEM (b) and spin wave excitation schematic (c)

Spin waves can also be excited by the spin-polarized currents injected into a ferromagnetic film due to the transfer of the spin-angular momentum as it was theoretically predicted [18, 19] and studied experimentally [20]. The interaction between spin waves and itinerant electrons is prominent near the interface between non-magnetic and ferromagnetic layers. The amplitude of the excited spin waves grows as the current density through the interface exceeds a certain critical value. This phenomenon

has been experimentally verified in Co/Cu multilayered structures showing high frequency 40–60 GHz current-driven spin wave excitation [21]. Spin wave excitation by the spin-polarized electric current has certain technological advantages and shortcomings. On one hand, spin wave excitation via spin torque requires only point contacts (characteristic size of the order of tens of nanometers), which is in favor of scalable devices. Geometry of the spin waveguide and properties of magnetic material used to fabricate

it determine the excited spin wave dispersion. Direct application of torque transferred by spin polarized electrons implies more efficient way of spin wave excitation while the giant magneto-resistance allows for a direct detection of local magnetization orientation at nano-scale, which is not possible with micro-strip antennas. On the other hand, the overall energetic efficiency may not be high. The threshold current density required for spin wave excitation is lower than $10^6 A/cm^2$, which is typically needed for a complete magnetization reversal. However, it is not clear how much of the consumed power can be transferred into a specific spin wave mode.

Another possible approach to the spin wave excitation and detection utilizes the local exchange fields that are effectively controlled in multiferroic elements. There is a growing interest in multiferroics – a special type of materials possessing electric and magnetic polarizations at the same time [22]. The electric and magnetic properties in multiferroics are related to each other via the internal magneto-electric coupling. It is possible to change magnetic polarization by electric field and vice versa. Multiferroics elements are of great promise as the possible input/output elements for spin wave devices enabling efficient energy conversion among the electric and magnetic domains. However, the most of the known room temperature multiferroics (i.e. $BiFeO_3$ and its derivatives [23]) are unlikely useful for spin wave excitation as they show a relatively small change of magnetization under the applied electric field. A new approach to the magnetization control via applied stress has been recently proposed and became known as the Hybrid Spintronics and Straintronics [24, 25]. The essence of this approach is in the use of two-phase composite multiferroics comprising piezoelectric and magnetostrictive materials, where an electric field applied across the piezoelectric produces stress, which, in turn, affects the magnetization of the magnetoelastic material. The advantage of this approach is that each material may be independently optimized to provide prominent electromagnetic coupling, which can be much higher than for a single-phase multiferroic [22]. There are several piezoelectric-piezomagnetic structures, which have been experimentally studied, showing a prominent magnetoelectric coupling: $PZT/NiFe_2O_4$ (1,400 mV cm^{-1} Oe^{-1}) [26], $CoFe_2O_4/BaTiO_3$ (50 mV cm^{-1} Oe^{-1}) [27], PZT/Terfenol-D (4,800 mV cm^{-1} Oe^{-1}) [28]. For instance, it was reported a reversible and permanent magnetic anisotropy reorientation in a magnetoelectric polycrystalline Ni thin film and (011)-oriented $[Pb(Mg_{1/3}Nb_{2/3})O_3]_{(1-x)}–[PbTiO_3]_x$ heterostructure

[25]. An important feature of the magneto-electric coupling is that the changes in magnetization states are stable without the application of an electric field and can be reversibly switched by an electric field near a critical value (i.e. 0.6 MV/m for Ni/PMN-PT). Such a relatively weak electric field promises an ultra-low energy consumption required for magnetization switching [29]. Synthetic multiferroics has been used for spin wave excitation/detection and have shown a reliable operation at room temperature [30].

Spin wave bus or spin waveguide is used to transfer the spin wave signal between the magnonic circuit elements [31, 32]. Its utility is similar to an optical waveguide aimed to guide the propagation of electromagnetic waves. The waveguide structure may consist of a magnetic film, a wire or a combination of wires made of ferromagnetic, antiferromagnetic, or ferrite material. Three different spin wave modes exist in thin ferromagnetic films: Magnetostatic Surface Spin Waves (MSSW), Backward Volume Magnetostatic Spin Waves (BVMSW), and Forward Volume Magnetostatic Spin Wave (FVMSW) dependent on the relative magnetization and spin wave wavevector orientation [33]. Patterning the ferromagnetic film into the wire-shaped structures enables spin wave guiding. Shape anisotropy of such structures defines the magnetization orientation, and enables support of finite non-zero frequency spin wave modes in the absence of biasing magnetic fields. As the magnetization aligns along the length of a ferromagnetic wire, the BVMSW modes traveling along the wire are excited. Excitation of MSSW and FMSW modes in magnetic wires requires substantial biasing external magnetic field or materials with high crystalline anisotropy for appropriate magnetization orientation. A traveling wave along the wire direction in combination with standing waves across the wire width and thickness result in existence of higher order BVMSW modes propagating with non-zero group velocities. Intrinsic non-linearity of spin waves in magnetic materials allows for inter-mode switching and parametric spin wave amplification [34] . The multimode spin waveguide operation allows for simultaneous independent information transmission in a different frequency bands. Figure 2 shows a typical dispersion of BVMSW modes in 1μm wide, 100nm thick CoTaZr waveguide. Spin wave dispersion is defined by the shape of the ferromagnetic wire and material parameters. The ratio of the spin waveguide width to its thickness defines the spin waveguide bandwidth with a highest frequency achieved in the waveguides with rectangular cross section for a given magnetic material [35, 36].
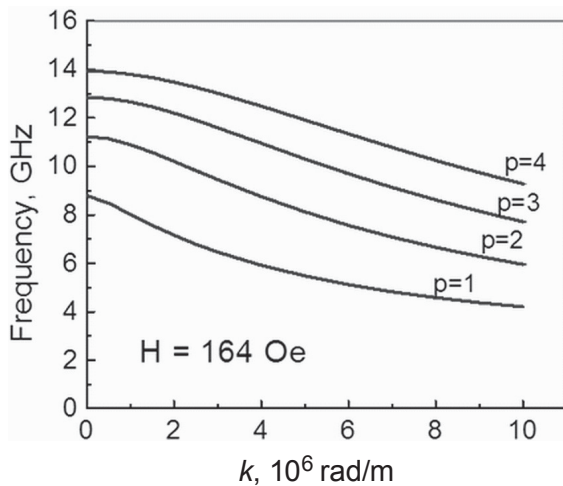
Fig. 2. Dispersion of the modes supported by magnetostatic backward volume waves for an ellipsoidal cross section with height to width ratio of ~1:10, saturation magnetization of ~1.2 T and an axial applied field of 164 Oe

Choosing the magnetic material plays crucial role in magnetic based logic devices as it determines the device performance parameters such as time per operation and gain (loss). Most of the magnetic logic devices utilize magnetization switching while spin wave logic rely on magnetic moment precession in magnetic material. The highest achievable frequency of magnetization switching occurs at ferromagnetic resonance (FMR) frequency. Frequency of operation should be much lower than the resonant frequency for reliable device performance. MSSW and FVMSW spin wave modes support higher than the FMR magnetization precession frequencies. Saturation magnetization of the magnetic material determines both the FMR and top of the magnetostatic spin wave band frequencies for a given shape of the magnetic material. Eddy currents in metallic ferromagnets and internal magnetization relaxation processes determine magnetization precession damping. The particular choice of a magnetic material for spin wave logic device will depend on many physical and technological conditions including its compatibility with silicon technology. Ferrimagnetic Yttrium Iron Garnet (YIG), $Y_3Fe_2(FeO_4)_3$ has a rich history of being a material of choice for microwave applications due to very low attenuation of magnetostatic magnetization oscillations [37]. However, low magnetization saturation of YIG limits the frequency range for which this material can be used. Ferromagnetic metals, such as Permalloy ($Ni_{81}Fe_{19}$), CoFe, $Co_{90}Ta_5Zr_5$ offer about one order of magnitude higher saturation magnetization supporting spin wave modes at much higher frequencies than

in YIG [38]. Both shape and crystalline anisotropy can be used to define the magnetization orientation at zero magnetic fields. These materials can be easily deposited using magnetron sputtering or electron beam evaporation techniques and patterned by standard nano-fabrication procedures to form spin wave busses as well as much more complex structures involved in magnetic logic and memory devices. Although eddy currents are the main source of high loss in the bulk ferromagnetic metals, small thicknesses of ferromagnetic films used in spin wave logic devices (less than 100–200nm, which is less than the skin depth) result in typical attenuation lengths in order of millimeters [13, 39]. Therefore the internal spin relaxation processes in these materials define the spin wave attenuation in micron- and nano-scale devices. Soft magnetic YIG and Permalloy are the two main candidates providing the desired frequency range which is further altered by engineering the shape of spin waveguides and other elements of spin wave logic devices.

As we mentioned above, spin wave propagation in patterned magnetic media is strongly dependent on its shape. Dependent on the shape of the structure and magnetization orientation different spin wave modes are supported. Spin waveguide shape alternations such as narrowing or widening [40], bending [41], local defects [42], air gaps [43, 44] (especially periodic air gaps in magnonic structures), material variation, and various junctions of three and more spin waveguides are essential for spin wave logic device construction. Any spin waveguide shape alternations results in a "defect" that causes spin wave scattering. Matching between the traveling spin wave modes supported by the spin waveguide and local spin wave modes of the "defect" defines the scattering process. By engineering the spin waveguide "defect" spin wave transmission, reflection or scattering at an angle into different spin waveguides (in case of spin wave junction) with shape-controllable spin wave amplitude and phase can be achieved. Alternation of spin wave modes in such "defects" in time domain using local magnetic fields or currents allows controlling the spin wave amplitude and phase as described in the sections below. Such spin wave propagation control forms the foundation for the spin wave logic device construction. Spin waveguide bend, essential for the spin wave logic device construction demonstrates such mode matching alternation (Figure 3) [41]. External uniform biasing magnetic field is used to magnetize the ferromagnetic wire perpendicularly to its axis enabling the MSSW mode transmission.
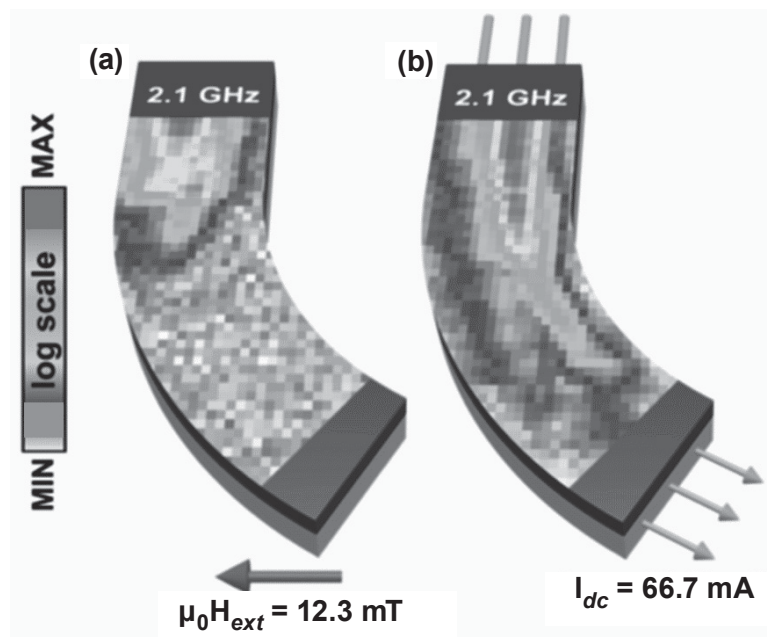
Fig. 3. Spin wave propagation through the spin waveguide bend. Hear shown
the spin wave intensity for uniform external magnetic field and oersted magnetic
field generated by underlying wire are applied

Alignment of magnetization along the field direction results in a different angle between the magnetization and the spin wave wave vector (propagation direction) in the area where the spin waveguide is bent. This results in local spin wave dispersion that differs from that in the straight spin waveguide. Spin wave mode mismatch prevents the spin wave transmission. When a DC current is driven though the highly conductive gold layer of the same shape as the incumbent magnetic spin waveguide oersted magnetic fields generated by such current magnetize the spin waveguide perpendicularly to its axis everywhere including the bend area. In this case the magnetization is aligned perpendicularly to the spin wave propagation direction even in the area of the waveguide bend. MSSW modes are supported in both the straight portion of the waveguide and in a bend allowing spin wave transmission.

The same physical principle of the spin wave scattering governs the spin wave scattering processes in a more complex structures such as a cross junction of two spin waveguides [45]. Shape anisotropy determines the axial magnetization alignment within a standing alone ferromagnetic wire. When two of such wires are brought together to form a ferromagnetic cross, the magnetization in the center of the cross junction aligns at 45º with respect to the cross arms while sufficiently long arms maintain axial magnetization. Figure 4 shows the results of

the micromagnetic simulations of the magnetization alignment in the junction of two spin waveguides crossed at 90º angle. In this structure the cross junction center plays a role of the local "defect" with misaligned magnetization. BVMSW modes excited in one of the cross arms propagate towards the center of the cross. Dependent on the magnetization orientation local standing spin wave modes are either excited or not in the ferromagnetic square that forms the junction. In contrast to the local spin wave modes intensively studied in standing alone square nano-magnets [46], the square in the cross center is subjected to non-uniform magnetic fields generated by the cross arms. Local standing spin wave modes in the center of the cross junction, if excited, in turn generate the outgoing spin waves in all four arms of the cross that form reflected and scattered waves. There are two interesting aspects of such spin wave scattering. Firstly, the spin wave scattering is strongly dependent on the magnetization orientation in the cross center. Variation of the latter results in different local spin wave modes which in turn affect the spin wave scattering. Spin wave scattering was studied experimentally and by numeric simulations in micron-scale CoTaZr cross. Spin waves were excited in the arm 1 of the cross and detected in arms 2–4 as a small external in-plane magnetic field was applied at a varying angle (as shown in Figure 4). External magnetic field was
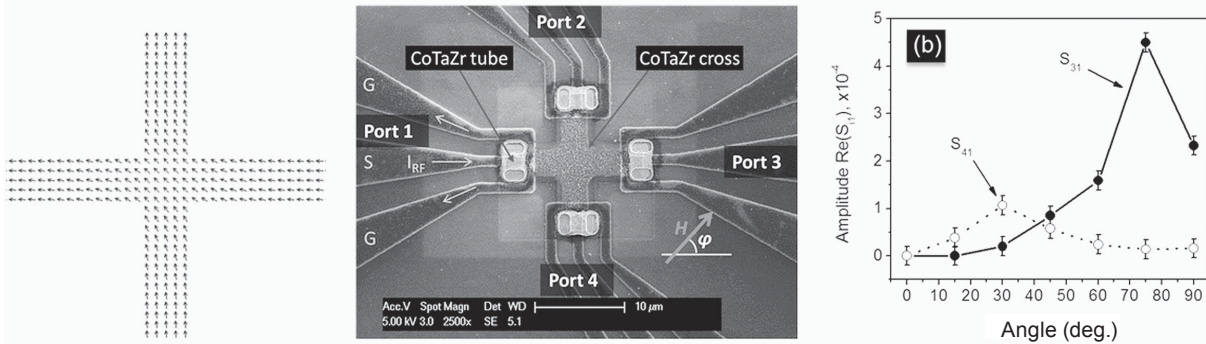
Fig. 4. Ferromagnetic cross junction. Micromagnetic simulation of the magnetization ground state (*left*); SEM micrograph of the cross junction test structure (*middle*); Amplitude of spin wave scattered into arms 3 and 4 of the cross shown in this figure (*right*)

small enough to ensure the axial magnetization within the cross arms. Amplitude of the scattered spin waves demonstrated strong dependence on the angle of the biasing field. At zero angles no spin wave transmission to the opposite arm of the cross was observed while there were spin waves scattered at 90 and 270 degree angles detected. As the field angle reached 45 degrees, almost equal spin wave scattering into all 3 output arms of the cross was observed. Further increase of the angle resulted in maximum transmission into the opposite arm while no scattering into the other two arms of the cross were observed. This effect can be utilized for spin wave switching by applying local magnetic fields to the cross junction center. Another striking phenomenon observed in ferromagnetic cross junction is the non-symmetric spin wave scattering. The wave scattered to the left arm gains different phase offset than the wave that scattered to the right. Non symmetry of spin wave scattering in the cross originates from the odd spin wave modes excited in the cross junction center. This phenomenon generates non-typical spin wave interference in this device which is described later in this chapter.

Air gaps introduced into the spin waveguides result in a similar defect that can be used to pre-program spin wave amplitude and phase changes in the magnonic circuit. Dipole-dipole interaction governs the magnetostatic spin wave propagation. Long range of dipolar forces allow spin wave propagation or as it is wrongly state "tunnel" though the dielectric gaps in the material [43, 44] as well as through the areas with local magnetization disorder [47, 48]. It was demonstrated that insertion of a dielectric gap affects the spin wave amplitude. The spin wave phase change is dependent on the gap width in comparison to the spin waveguide cross section dimensions. Similar effect is observed in the areas

with field controlled local magnetization disorder. Spin wave "tunneling" through a dielectric gap allows electrically isolating selected parts of the spin waveguide. Spin waveguide electrical isolation plays a very important role in the proposed magnonic logic devices as it allows driving local currents through the parts of the waveguide (e.g. when using spin torque devices) and applying local magnetic fields without affecting the spin wave propagation. Periodic air gaps introduced into the spin waveguide results in formation of so called magnonic crystal. Periodic patterning of magnetic films results in the band-gap opening (magnonic gap) in the spin wave energy spectrum that combines delocalized traveling spin wave modes and local standing spin waves. Similar spin wave dispersion modifications can be made by introducing periodic defects in the spin waveguide such as holes, thickness and material variations. Detailed review of such structures can be found in the literature [49]. Besides the pre-designed spin waveguide shape and material property variations spin wave dispersion can be altered by introducing controllable local magnetization disorders. Such disorders allows for a controllable spin wave amplitude and phase variations that are required in all magnonic logic devices.

Some types of spin wave logic devices require a special element − a phase modulator, aimed to provide a π-phase shift to the propagating spin wave. The operation of the interferometer-based logic devices [50–52] depends on this element. A reconfigurable magnonic circuits would also require such an element [14]. The main requirements for the phase modulator are scalability and low power consumption. Phase modulation is achieved by the applying of the local magnetic field affecting the dispersion of the propagating spin wave. In general, such an element can be realized as a static (delay line, perma-

nent magnet, domain wall) or dynamic (conducting contour) elements. The use of external magnetic field produced by an electric current in the conducting substrate may not be efficient from this point of view. Scaling down of the interferometer dimensions will require an increase of the electric current to provide stronger magnetic field. This problem may be solved in part by using the optimized structure presented in Ref. [52]. It should be noted that the phase shifters used in the interferometer-based circuits [52] and shifters used for circuit reconfiguration [14] have different operation frequency. The shifters used in the interferometers-based switches may be needed in every computational step and have to sustain high-frequency operation. In contrast, circuit reconfiguration occurs on a much longer time scale. In this case, a non-volatile element such as a domain wall can be used to provide constant phase shift without the use of an external power.

2. Magnonic Logic Devices

There are three basic approaches to magnonic logic devices, which are defined by the method of information encoding into the spin waves. Logic zeroes and ones can be assigned to i) the amplitude (10–12), (ii) the phase (13), or (iii) the frequency (14) of the spin wave signal. The method of information encoding is very important as it further defines the principle of operation of the basic logic gates, the design and the computing capabilities of the architecture solutions. For example, encoding information into the amplitude of the spin wave signal (10–12), where logic 0 and 1 correspond to the two spin wave amplitudes. The schematics of the amplitude-based magnonic logic gates are shown in Figure 5. The main building block is a miniature Mach–Zehnder interferometer with a vertical current-carrying wire. The area of the interferometer can be as small as 300nm × 300nm. With a zero current applied, the spin waves in two branches interfere constructively and propagate through. The waves interfere destructively and do not propagate through the structure if a certain electric current I_π is applied. The complete set of logic gates (i.e. NOT, NOR, NAND) can be built by integrating the Mach–Zehnder interferometers as proposed in Ref. [52]. It should be noted, that in the considered scheme the input logic state is represented by the amplitude of the electric current and the output state is assigned to the amplitude of the spin wave signal A, which implies an
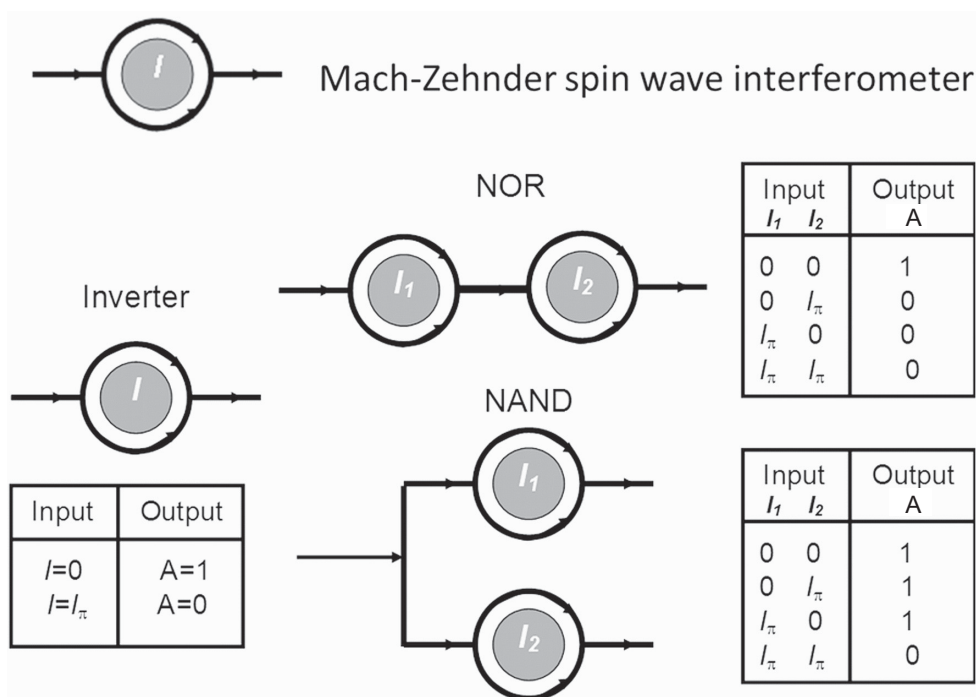

Fig. 5. Schematics of the amplitude-based spin wave logic devices. The basic element is the Mach–Zehnder-type spin wave interferometer. The phase shift in one of the interferometer's arms is controlled by the magnetic field produced by an electric current I. A set of logic gates (NOT, AND, OR) for general type computing built with the Mach–Zehnder interferometers. A bit of information is assigned to the amplitude of the propagating spin wave A (i.e. Logic 1 corresponds to some A>0, and logic 0 corresponds to A=0)

additional element for spin wave to electric current conversion. At some point, this device resembles the classical field effect transistor, where the magnetic field produced by the electric current modulates the propagation of the spin wave- an analog to the electric current. One hand, this approach can benefit of the well-defined methodology for Boolean-type logic gate construction. On the other hand, it cannot offer any fundamentally more advantageous alternative to the existing CMOS-based logic circuitry.

In the phase-based approach, logic 0 and 1 are assigned to the phase (0 or π) of the propagating spin wave [31]. The principle of operation of the phase-based magnonic logic circuit is fundamentally different from the conventionally adopted field-modulated amplitude approach. Within this approach, a bit of information is assigned to the phase of the propagating spin wave. An elementary act of computation is associated with the change of the phase of the propagating spin wave. The latter provides an alternative route to the NOT and Majority logic gate construction. The schematics of the phase-based magnonic logic circuit are shown in Figure 6.

voltage	phase
+ 10mV	0
- 10mV	π

A	B	C	Junction	Inverter
0	0	0	0	π
0	0	π	0	π
0	π	0	0	π
0	π	π	π	0
π	0	0	0	π
π	0	π	π	0
π	π	0	π	0
π	π	π	π	0

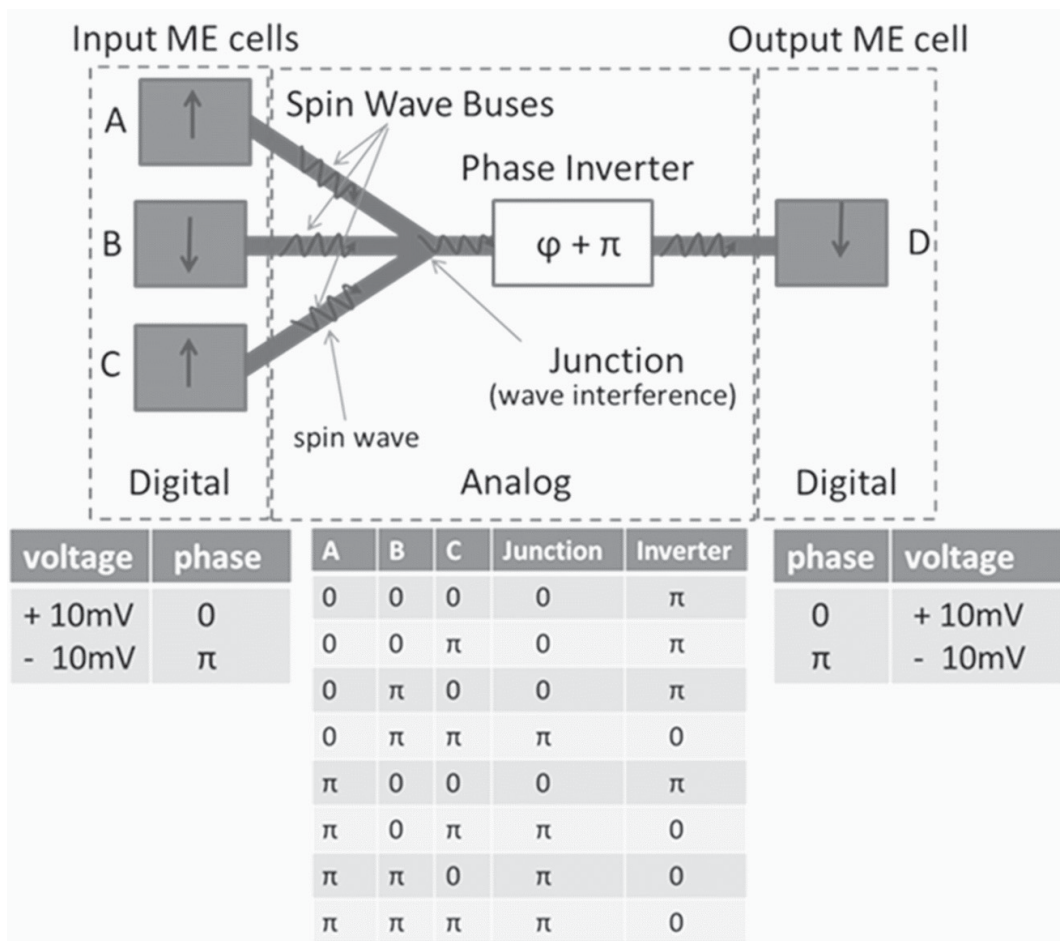| phase	voltage
0	+ 10mV
π	- 10mV

Fig. 6. Schematic view of the spin wave logic circuit. There are three inputs (A,B,C) and the output D. The inputs and the output are the ME cells connected via the ferromagnetic waveguides – spin wave buses. The input cells generate spin waves of the same amplitude with initial phase 0 or π, corresponding to logic 0 and 1, respectively. The waves propagate through the waveguides and interfere at the point of junction. The phase of the wave passed the junction corresponds to the majority of the interfering waves. The phase of the transmitted wave is inverted (e.g. passing the domain wall). The Table illustrates the data processing in the phase space. The phase of the transmitted wave defines the final magnetization of the output ME cell D. The circuit can operate as NAND or NOR gate for inputs A and B depending the third input C (NOR if C=1, NAND if C=0)

The circuit comprises the following elements: (i) magneto-electric cells, (ii) magnetic waveguides – spin wave buses, and a (iii) phase shifter. Magneto-electric cell (hereafter, ME cell) is the element aimed to convert applied voltage into the spin wave as well as to read-out the voltage produced by the spin waves (i.e. a two-phase multiferroic as described in the preceding Section). The operation of the ME cell is

based on the effect of the magneto-electric coupling (i.e. multiferroics) enabling magnetization control by applying an electric field and vice versa. The waveguides are simply the strips of ferromagnetic material (e.g. NiFe) aimed to transmit the spin wave signals. The phase shifter is a passive element (e.g. the same waveguide of different width, a domain wall) providing a π-phase shift to the propagating spin waves.

The principle of operation is the following. Initial information is received in the form of voltage pulses. Input 0 and 1 are encoded in the polarity of the voltage applied to the input ME cells (e.g. +10mV correspond to logic state 0, and -10mV correspond to logic 1). The polarity of the applied voltage defines the initial phase of the spin wave signal (e.g. positive voltage results in the clockwise magnetization rotation and negative voltage results in the counter clockwise magnetization rotation). Thus, the input information is translated into the phase of the excited wave (e.g. initial phase 0 corresponds to logic state 0, and initial phase π corresponds to logic 1). Then, the waves propagate through the magnetic waveguides and interfere at the point of waveguide junction. For any junction with an odd number of interfering waves, there is a transmitted wave with non-zero amplitude. The phase of the wave passing through the junction always corresponds to the majority of the phases of the interfering waves (for example, the transmitted wave will have phase 0, if there are two or three waves with initial phase 0; the wave will have a π-phase otherwise). The transmitted wave passes the phase shifter and accumulates an additional π-phase shift (i.e. phase $0 \rightarrow \pi$, and phase $\pi \rightarrow 0$). Finally, the spin wave signal reaches the output ME cell. The output cell has two stable magnetization states. At the moment of spin wave arrival, the output cell is in the metastable state (magnetization is along the hard axis perpendicular to the two stable states). The *phase* of the incoming spin wave defines the direction of the magnetization relaxation in the output cell [14, 53]. The process of magnetization change in the output ME cell is associated with the change of electrical polarization in the multiferroic material and can be recognized by the induced voltage across the ME cell (e.g. +10mV correspond to logic state 0, and -10mV correspond to logic 1). The Truth Table inserted in Figure 2 shows the input/output phase correlation. The waveguide junction works as a Majority logic gate. The amplitude of the transmitted wave depends on the number of the in-phase waves, while the phase of the transmitted wave always corresponds to the majority of the phase inputs. The π-phase shifter

works as an Inverter in the phase space. As a result of this combination, the three-input one-output gate in Figure 2 can operate as a NAND or a NOR gate for inputs A and B depending on the third input C (NOR if C=1, NANrisD if C=0). Such a gate can be a universal building block for any Boolean logic gate construction. Computing with phases has certain fundamental advantages over the conventional amplitude-based approach. For example, the utilization of wave interference makes it possible to build certain types of logic gates (e.g. MAJ, MOD [53]) with fewer number of elements. Even more important are the advantages of using spin wave superposition for building multi-channel logic gates [54], which offer an alternative route to functional throughput enhancement.

Frequency-based magnonic circuits have been recently proposed (14). The proposed circuits consist of the spin torque oscillators communicated via spin waves propagating through the common free layer. This approach is based on the property of nanometer scale spin torque devices generate spin waves in response to a d.c. electrical current (18, 19). Electric current passing through a spin torque nano-oscillator (STNO) generates spin transfer torque and induces auto-oscillatory precession of the magnetic moment of the spin valve free layer. The frequency of the precessing magnetization is tunable by the applied dc voltage due to the strong non-linearity of the STNO. In case of two or more STNOs sharing a common free layer, the oscillations can be frequency and phase locked via the spin wave exchange (20, 21). The schematics of the MAJ logic gate based on the phase locking of STNOs with a common free-layer metallic ferromagnetic nanowire are shown in Figure 7. The gate has three inputs and one output. All inputs are dc current-biased at a current level above the critical current for magnetization self-oscillations. To each input, signals of two frequencies f_1 and f_2 can be applied. Due to injection locking and spin wave interaction in the common free layer, the entire free layer precesses at either f_1 or f_2, depending on the input signal frequency applied to the majority of the inputs. Therefore, the output frequency of this logic gate is determined by the frequency applied to the majority of the input gates, and the device operates as a majority logic gate with the signal frequency as the state variable [55]. The unique properties of STDs are of great promise for future implementation. Being compatible with CMOS, STDs may serve as complementary logic units for general and special task data processing. The main challenge for the STD approach is to reduce the current required for switching and minimize active power consumption.
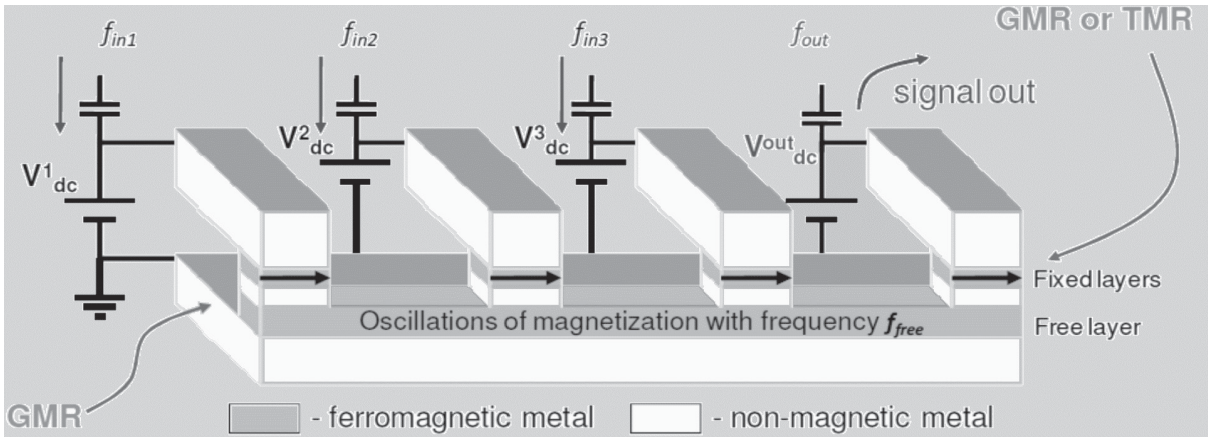
Fig. 7. Schematics of the STO-based MAJ logic gate consisting of a metallic ferromagnetic nanowire with several injectors of spin polarized current (spin toque oscillators with a common free layer). The input frequencies (e.g. f_1, f_2, f_3) assume binary values. The output frequency fout in the phase locking regime is determined by the majority of the input frequencies

It has been a lot of progress in the experimental demonstration of spin wave components and the prototyping of complete magnonic logic gates during the last decade. The first working spin-wave based logic device has been experimentally demonstrated by M. P. Kostylev et al. [50]. The authors used Mach–Zehnder-type current-controlled spin wave interferometer to demonstrate output voltage modulation as a result of spin wave interference. This first working prototype device was of a great importance for the development of magnonic logic devices. The device show reliable operation in the GHz frequency range and at room temperature, which immediately made it a favorite among the other proposed spin-based logic devices. Later on, exclusive-not-OR and not-AND gates have been experimentally demonstrated on a similar Mach–Zehnder-type structure [51].

Next, there were realized three- and four-terminal spin wave prototypes. Figure 8 shows the schematics of the four-terminal spin wave device used as a prototype for the MAJ gate [56]. The material structure from the bottom to the top consists of a silicon substrate, a 300nm thick silicon oxide layer, a 20nm thick ferromagnetic layer made of $Ni_{81}Fe_{19}$, a 300nm thick layer of silicon oxide and the set of five conducting wires on top. The distance between the wires is 2μm. In order to demonstrate a three-input one-output majority gate, three of the five wires were used as the input ports, and two other wires were connected in a loop to detect the inductive voltage produced by the spin wave interference. An electric current passing through the "input" wire generates a magnetic field, which, in turn, excites spin waves in the ferromagnetic layer. The direction of the current flow (the polarity of the applied voltage) defines the initial spin wave phase. The curves of different numbers in Figure 8
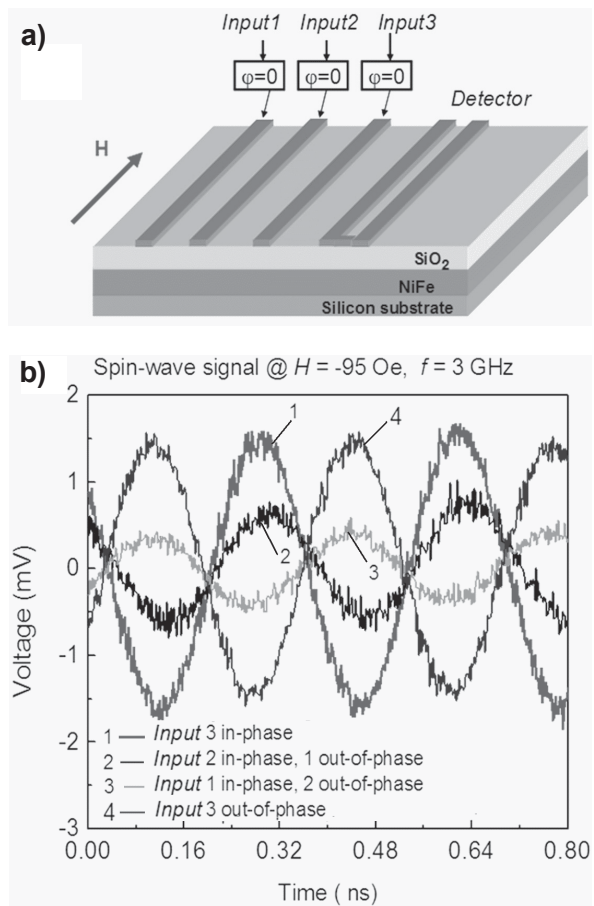

Fig. 8. (a) Schematics of the 4-terminal SWD. The device structure comprises a silicon substrate, a 20nm thick layer of permalloy, a layer of silicon dioxide, and a set of five conducting wires on top (three wires to excite three spin waves, and the other two wires connected in a loop are to detect the inductive voltage). The initial phase of the excited spin wave (0 or p) is controlled by the direction of the excitation current. (b) Experimental data showing the inductive voltage as a function of time. The curves of different number correspond to the different combinations of the phases of the interfering spin waves

depict the inductive voltage as a function of time for different combinations of the spin wave phases (e.g. 000, 0π0, 0ππ and πππ). These results show that, the phase of the output inductive voltage corresponds to the majority of the phases of the interfering spin waves. Spin waves produce several mV of inductive voltage output with signal to noise ratio about 10:1. The data are taken for 3GHz excitation frequency and at bias magnetic field of 95Oe (perpendicular to the spin wave propagation). All measurements were accomplished at room temperature.

The use of electric-current wires for spin wave excitation appeared to be energetically inefficient (i.e. > pJ per spin wave), as only a small amount of energy is transferred into the spin wave. It would be much more efficient to utilize multiferroics for energy conversion among the electric and magnetic domains [57].

Recently, spin wave excitation and detection by synthetic multiferroic elements has been experimentally demonstrated [16]. The schematics of the experiment and experimental data are shown in Figure 9. Two synthetic multiferroic elements were
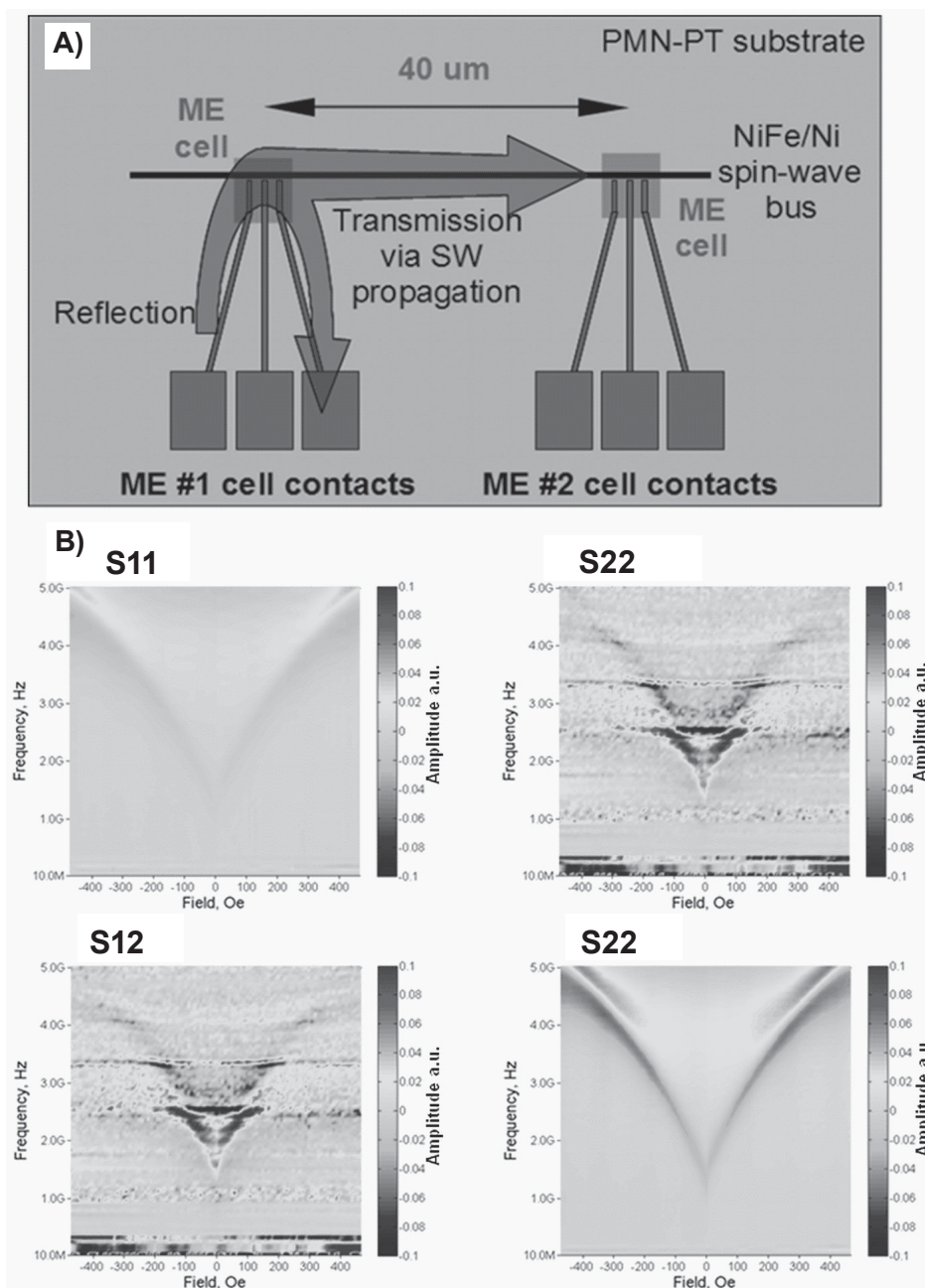

Fig. 9. (A) Schematics of the experiment on spin wave excitation and detection by multiferroic elements (ME cells). (B) Collection of the experimental data (S11, S12, S21 and S22 parameters) obtained at different frequencies and bias magnetic field

used to excite and detect spin wave propagating in the permalloy waveguide (the distance among the excitation and the detection elements is 40μm). The multiferroic element comprises a layer of piezoelectric (PZT) and a magnetostrictive material (Ni). An electric field applied across the piezoelectric produces stress, which, in turn, affects the magnetization of the magnetostrictive material. Thus, the applying of AC voltage to the multiferroic element results in the magnetization oscillation (spin wave). And vice versa, the change of magnetization in the magnetostrictive layer results in the voltage signal due to the produced stress. The experimental data in Figure 9(b) show the collection of data obtained at different operational frequencies and bias magnetic field. The utilization of multiferroics has resulted in the energy reduction to about 10fJ per wave [16]. Most of the currently proposed magnonic logic devices are designed to perform a single logic operation. All of them except for the STNO majority logic device share the following signal processing flow for the spin wave logic gate operation: 1) Input electrical signal (either current or voltage) is used to excite a spin wave (pulse or in CW regime); spin wave phase is used to carry the information. 2) Spin waves travel to the area where interference of two or more waves is happening; 3) constructive or destructive interference defines the output wave amplitude; 4) the output wave amplitude (if any) is converted to the electronic signal. Spin wave phase carries the input information while the wave amplitude is used to represent the output information. In order to build logic based on such spin wave gates a spin wave amplitude-to-phase convertor is required. In most cases a conventional electronics is implied to detect

the spin wave, and adjust the phase of the spin wave input of the next spin wave logic gate. Therefore most of the proposed spin wave logic gates cannot be used as a building block for spin wave logic circuit construction without using intermediate electronic stages. In case of destructive interference the wave phase information is lost – another obstacle that can be addressed by feeding the reference wave into the every intermediate stage between the logic gates. Without electronic components, such logic gates can operate only as a standing alone signal processing devices and cannot be assembled into logic circuits. Unique spin wave scattering in the ferromagnetic cross junction provides a convenient tool to address this problem as follows [58]. Ferromagnetic cross has 4 arms labeled as ports 1 through 4 (see Figures 4 and 10). Ports 1 and 2 are used as inputs and ports 3 and 4 – as outputs. Spin waves excited in ports 1 and 2 are traveling towards the cross center where they experience scattering on the center of the junction. Scattered waves interfere in the cross arms 3 and 4. The spin waves scattered at ±90º (into the neighboring arms of the cross) gain different phase offsets. As the phase of the spin wave in port 2 is linearly changed, spin wave amplitude oscillation is detected in ports 3 and 4 (see Figure 10). Despite the geometrical symmetry of the structure, spin wave interference is not symmetrical (constructive and destructive interference in the output arms 3 and 4 is not happening at the same phase offsets of the input spin waves). Non-symmetric phase gain of the scattered spin wave modes at the central part of the cross junction define the wave propagation and is responsible for the interference that was observed experimentally. Numeric simulations confirm the
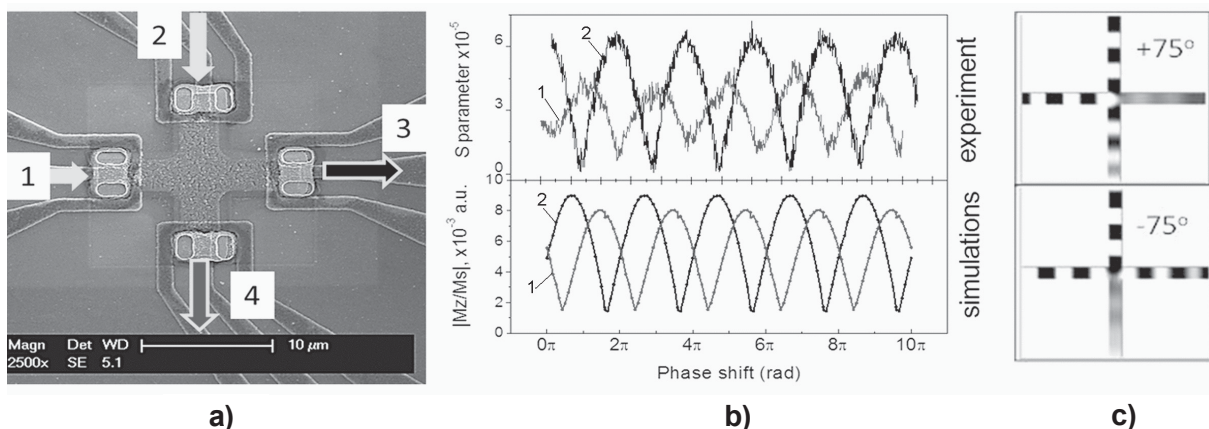

Fig. 10. (a) Cross junction structure SEM micrograph indicating input and output spin wave signals. (b) Spin wave interference in ferromagnetic cross junction: output wave amplitude dependence on the input waves phase offset (experiment and micromagnetic simulations; 1 – S41, 2 – S31) (c) Micromagnetic simulation of the spin wave interference: destructive interference in the output arms 3 and 4 (phase +75º for output 3 and -75º for the output 4)

significance of the central region design. The spin wave scattering becomes symmetrical when the central part of the cross junction is removed (4 waveguides with no central rectangle) thus demonstrating the effect of local spin wave mode interaction with the traveling spin waves, causing non-symmetric spin wave scattering. In case of the empty cross junction symmetric spin wave scattering is caused by spin wave "tunneling" [47] through the central part. In this case the symmetry of the cross arm alignment defines the interference pattern in the cross output arms. The interference of two waves in ferromagnetic cross is unique as for all input spin wave phase shifts there is an output spin wave non-zero amplitude detected either in port 3 or port 4. The output spin waves of this device can be merged to form a single device output as shown in Figure 11. The spin wave phases of zero and φ_0 (with respect to the reference) encode logical "0" and "1". The value φ_0 defines the condition for destructive interference in one of the arms of the

cross. It is strongly dependent on the cross junction geometry and in case of the cross shown in figure 10 φ_0=75°. Cross output waves will either scatter to one or another arm of the cross for the (0, 1) and (1, 0) or to the both arms simultaneously for (0, 0) and (1, 1) input signal configurations. The phases of the output waves measured at the cross arms 3 and 4 and will have phases shown in the table in Figure 11. The spin waves in the cross arm 3 and 4 are then merged ensuring the constructive spin wave interference. The spin wave phase in the output waveguide at the merge point will follow the OR logic operation. The φ_0 phase shift produced either by the delay line or externally controlled phase shifter will act as an inverter. This will result in the output wave following NOR logic operation. Knowledge of the local spin wave modes in the spin waveguide junction should allow for multi-terminal spin wave devices where the output wave phase shift is defined by the phase gains of the spin waves scattered in the junction.

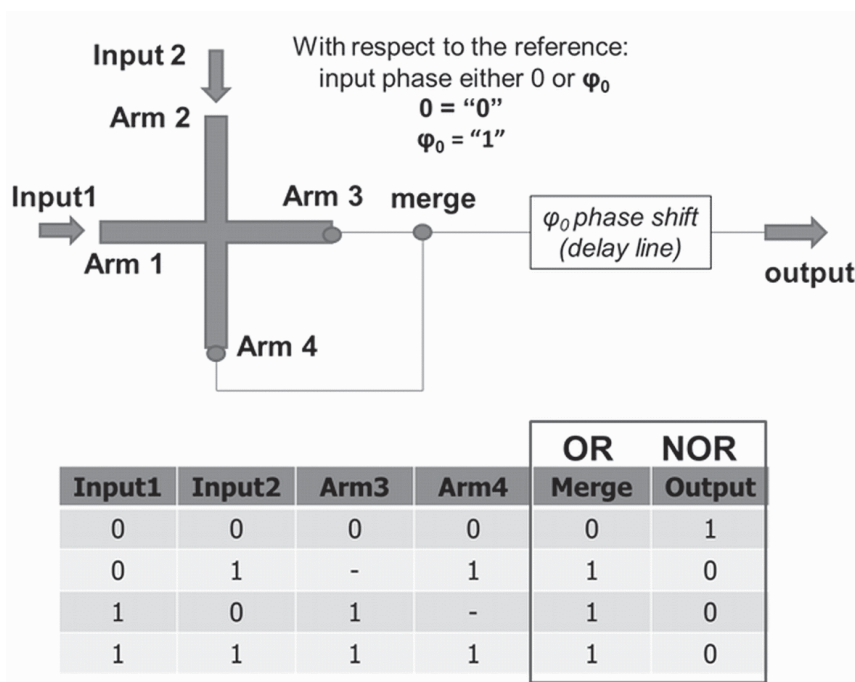| Input1	Input2	Arm3	Arm4	OR Merge	NOR Output
0	0	0	0	0	1
0	1	-	1	1	0
1	0	1	-	1	0
1	1	1	1	1	0

Fig. 11. Spin wave OR/NOR logic gates based on ferromagnetic cross junction. Device schematic (top) and truth table (bottom). Dash in the table indicates zero wave amplitude

Recently, a prototype comprising two cross junctions has been realized. The schematics of the test structure and experimental setup are shown in Figure 12. The double-cross structure is made of yttrium iron garnet $Y_3Fe_2(FeO_4)_3$ (YIG) epitaxially grown on gadolinium gallium garnet $Gd_3Ga_5O_{12}$ substrate with (111) crystallographic orientation.

YIG film has ferromagnetic resonance (FMR) linewidth $2\Delta H \approx 0.5 Oe$, saturation magnetization $4\pi M_s$=1750G, and thickness d=3.6µm. The length of the whole structure is 3mm, the width of the arm in 360µm. There are six micro-antennas fabricated on the top of the YIG waveguides. These antennas are used to excite spin wave in YIG material and to
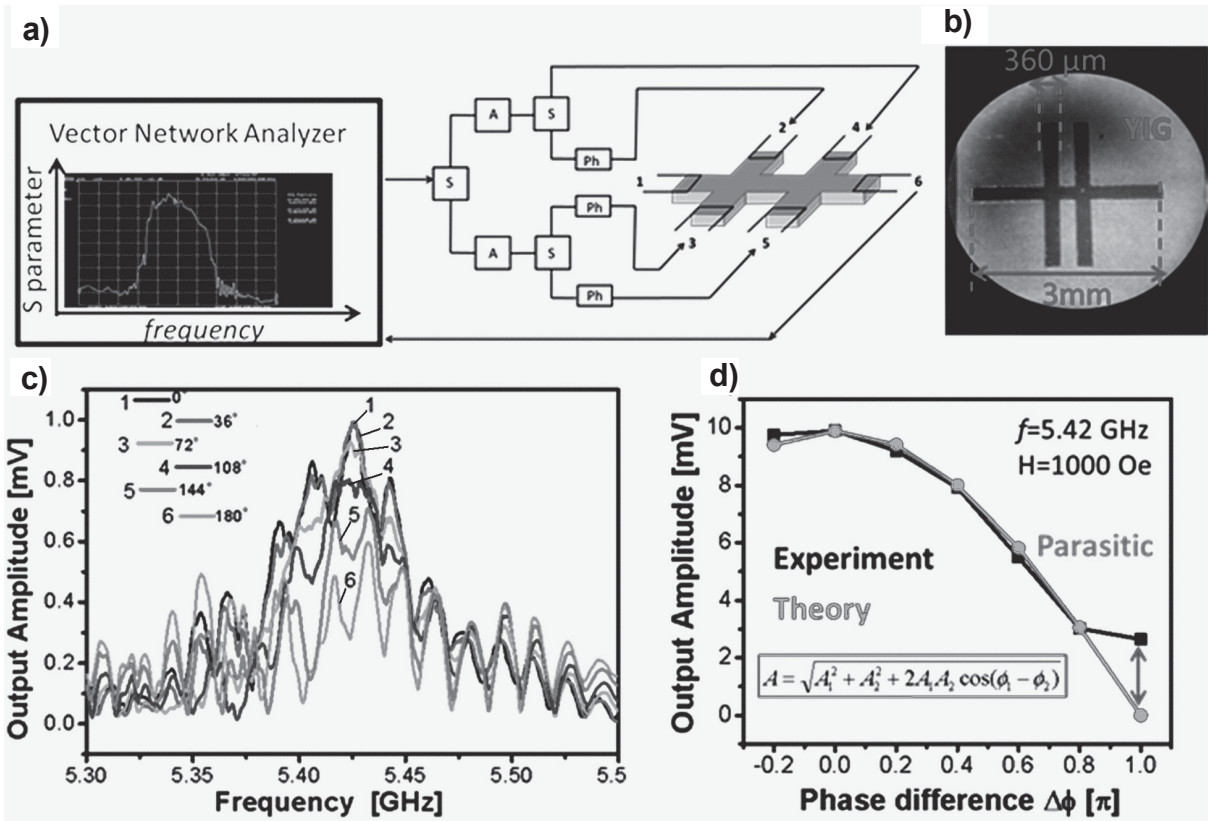
Fig. 12. (a) The schematics of the experimental setup. The test under study is a double-cross YIG structure with six micro-antennas fabricated on the edges. The input and the output micro-antennas are connected to the Hewlett-Packard 8720A Vector Network Analyzer (VNA). The VNA generates input RF signal in the range from 5.3GHz to 5.6GHz and measures the S parameters showing the amplitude and the phases of the transmitted and reflected signals. (b) The photo of the YIG double-cross structure. The length of the structure is 3mm, and the arm width is 360μm. (c) Transmitted signal S12 spectra for the structure without micro-magnets. Two input signals are generated by the micro-antennas 2 and 3. The curves of different namber show the output inductive voltage obtained for different phase difference among the two interfering spin waves. (d) The slice of the data taken at the fixed frequency of 5.42GHz (black curve). The red curve shows the theoretical values obtained by the classical equation for the two interfering waves.

detect the inductive voltage produced by the propagating spin waves. The input and the output micro-antennas are connected to the Hewlett-Packard 8720A Vector Network Analyzer (VNA). The VNA generates an input RF signal up to 20 GHz and measures the S parameters showing the amplitude and the phases of the transmitted and reflected signals. The prototype is placed inside an electro-magnet allowing variation in the bias magnetic field from -1000Oe to +1000Oe. The input from VNA is split between the four inputs via the two splitters, where the amplitudes of the signals are equalized by the attenuators (step ±1dB). The phases of the signal provided to the ports 3 and 4 are controlled by the two phase shifters (±2^0). The photo of the YIG structure is shown in Figure 12(B). The graph in Figure 12(C) shows the amplitude of the output inductive voltage detected for different excitation frequencies in the range from 5.30GHz to 5.55GHz. The curves

of different numbers depict the output obtained for different phase difference $\Delta\varphi$ among the two inputs 2 and 3. These data show the oscillation of the output voltage as a function of frequency and the phase difference between the two generated spin waves. The frequency dependence of the output is attributed to the effect of spin wave confinement within the structure, while the phase-dependent oscillations reveal the interference nature of the output signal. In Figure 12 (D), we show the slice of the data taken at the fixed frequency of 5.42GHz. The experimental data has a good fit with the classical equation for the two interfering waves. The only notable discrepancy is observed for $\Delta\varphi=\pi$, where experimental value is non-zero. This fact can be well understood by taking into account all possible parasitic effects (e.g. reflecting waves, direct coupling between the input/output ports, structure imperfections, etc.)

3. Spin wave-based logic gates and architectures

Since the first proposal on spin wave logic [31], there have been a number of works, where the idea of using spin waves in logic circuitry has been evolved in different ways [14, 53, 54, 59]. The variety of possible spin wave based devices can be classified within several groups including single-frequency and multi-frequency, Boolean and non-Boolean, volatile and non-volatile circuits. For example, logic devices shown in Figures 5, 6, and 8 use one operating frequency and constitute the group of single-frequency logic devices. There may be more than one operating frequency per device (e.g. the device shown in Figure 7), which entitled the group of multi-frequency devices. At the same time, single and multi-frequency devices may be used for building Boolean and non-Boolean type of logic gates. Boolean magnonic circuits are aimed to provide the same basic set of logic gates (AND, OR, NOT) for general type computing as provided by the conventional transistor-based circuit. The advantage of using waves (i.e. spin waves) is the ability to exploit the waveguides as passive logic elements for controlling the phase of the propagating wave. Waveguides of the same length but different width, or composition introduce different phase change to the propagating spin waves. The latter offers an additional degree of freedom for logic circuit construction. Besides that, the utilization of spin wave interference is efficient for building high fan-in devices, which is a significant advantage over the transistor-based circuits [56]. Overall, magnonic Boolean logic circuits can be constructed with a fewer number of elements that it is required for CMOS counterparts [60]. This advantage is more prominent for complex logic circuits. For example, magnonic Full Adder Circuit cab be built with just 5 ME cell, while the conventional design requires at least 25 transistors [53].

Non-Boolean magnonic circuits constitute a novel direction for magnonic circuit development aimed to complement scaled CMOS in special task data processing. In contrast to the Boolean logic gates for general type data processing, non-Boolean circuits are designed for one or several specific logic operations. Data search and image processing are the examples of widely-used tasks, which require significant amount of resources from a general type processor. Parallel data processing of a large number of bits can be accomplished by utilizing a multi-wave interference, where each wave (i.e. the phase of the wave) represents one bit of data. The examples of non-Boolean magnonic logic circuits for pattern recognition, finding the period of a given function, and magnonic holographic memory are described in Ref. [61]. The operation of these circuits is based on the massive use of spin wave interference within a magnetic template. This approach is similar to the methods developed for "all optical computing" [62], though the practical implementation of the magnonic circuits may be more feasible for integration on the silicon platform.

The above mentioned groups of magnonic logic devices may be volatile or non-volatile. Volatile magnonic circuits provide functional output (i.e. inductive voltage) as long as external power is applied to the spin wave generating elements [30] or spin wave buses are combined with an electric circuit preserving the output voltage produced by the spin wave pulses [59]. For example, magnonic circuits described in Ref. [14] combine spin wave buses with micro antennas. The circuit operates as long as the input antennas generate continuous spin waves. It is also possible to build a circuit combining spin wave buses with a bi-stable electric circuit, where the switching of the electric circuit is accomplished by the inductive voltage pulse [59]. In this case, there no need in permanently spin wave generating elements, though external power is required to maintain the state of the electronic circuit. Non-volatile magnonic logic circuits are able to preserve the result of computation without external power applied. The storing of information is in the magnetic state of the output ME cell, where logic 0 and 1 are encoded into the two states of magnetization of the magnetostrictive material [53]. In general, magnetic field produced by a spin wave is quite weak to reverse the magnetization of a large volume ferromagnetic required for reliable data storage (thermal stability >40). The switching is accomplished via the help of magneto-electric coupling, where an electric field applied to ME cell rotates its magnetization in a metastable state, and then, incoming spin wave defines the direction of relaxation [53]. Non-volatile magnonic logic devices have been recognized as one of the promising approaches to post-CMOS circuitry for radical power consumption minimization [63].

We would like specially outline the possibility of building multi-frequency magnonic logic circuits, aimed to the advantage of wave superposition for functional throughput enhancement. Multi-frequency magnonic logic circuits are the circuits using more than one operating frequency for data transmission and processing. Wave superposition

allows us to send, process, and detect a number of waves propagating within the same structure at a time. The general view of the multi-frequency magnonic circuit as described in Ref. [54] is shown in Fig.13. The structure and the principle of operation are similar to the above described example (see Figure 6) except there are multiple ME cells on each of the input and output nodes. These cells are aimed to operate (excite and detect) spin waves on different frequencies (e.g. $f_1, f_2, ..., f_n$). Each of the frequencies $\{f_1, f_2, ..., f_n\}$ is considered as an independent information channel, where logic 0 and 1 are encoded into the phase of the propagating spin wave. The frequency excited by the ME cell depends on many factors and can be adjusted by the cell size/shape/composition. In order to avoid the crosstalk among the cells operating on different frequencies, the cells are connected with the spin wave buses via the magnonic crystals [64] serving as frequency filters. Each of these crystals allows spin wave transport within a certain frequency range enabling ME cell frequency isolation. Within the spin wave buses, spin waves of different frequencies superpose, propagate, and receive a π-phase shift independently of each other. Logic 0 and 1 are encoded into the phases of the propagating spin waves on each frequency. The output ME cells are connected to the spin wave buses via the magnonic crystals in order to receive spin wave signal on the specific frequency. The Truth Table shown in Figure 6 can be applied for the each of the operating frequencies. Thus, the considered circuit can perform NAND or NOR operations on the number of bits at the same time. The multi-frequency approach is an extension that can be applied to the all types of magnonic circuits described above.
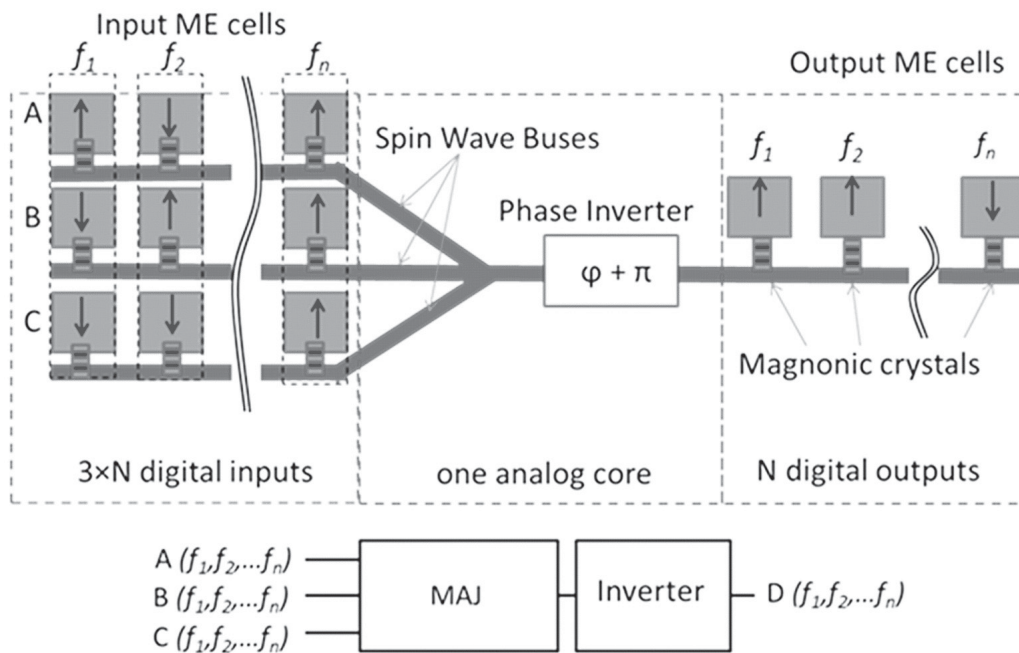

Fig. 13. Schematic view of the multi-frequency magnonic circuit. There are multiple ME cells on each of the input and output node aimed to excite and detect spin waves on the specific frequency (e.g. $f_1, f_2, ..., f_n$). The cells are connected to the spin wave buses via the magnonic crystals serving as the frequency filters. Within the spin wave buses, spin waves of different frequencies superpose, propagate, and receive a π-phase shift independently of each other. Logic 0 and 1 are encoded into the phases of the propagating spin waves on each frequency. The output ME cells recognize the result of computation (the phase of the transmitted wave) on one of the operating frequency (2012)

The ability to use wave interference and the integration of spin wave buses with non-linear magnetic elements (e.g. multiferroic cell serving as a memory and data processing unit at the same time) opens intrigue possibilities for building non-Boolean logic gates and complex computational architectures such as Cellular Nonlinear Network (CNN) [65] and Holographic Computing [66]. CNN was first formulated by Leon Chua [65] as a 2 (3 or more) dimensional array of mainly identical dynamical systems, called cells, which satisfy two properties: (i) most interactions are local within a finite radius

R, and (ii) all state variables are signals of continuous values. In the series of subsequent works, the CNN paradigm was evolved in many ways and powerful computing abilities of the CNN, especially for image processing, were demonstrated [67–70]. Nowadays, the CNN has been received a growing deal of interest as a promising architecture for future computation using nanosclae devices and structures. The utilization of spin waves together with multiferroic elements offers an original route to magnonic network, where communication between the multiferroic cells is via spin waves [71]. The schematic of the magnonic CNN is shown in Figure 14(a). The network consists of magneto-electric cells integrated onto a common ferromagnetic film–spin wave bus. The magneto-electric cell is the same as the described earlier in the text. It comprises piezoelectric and ferromagnetic materials, where a bit of information is assigned to the cell's magnetic polarization. The information exchange among the cells is via the spin waves propagating in the spin wave bus. Each cell changes its state as a combined effect: magneto-electric coupling and the interaction with the spin waves. The distinct feature of the network with a spin wave bus is the ability to control the inter-cell communication by an external global parameter — magnetic field. The latter makes it possible to realize different image processing functions on the same template without rewiring or reconfiguration. In Figure 14(b), there are shown the examples of image processing

functions dilation and erosion accomplished at two different magnetic bias fields. More complex image processing functions such as vertical and horizontal line detection, inversion, and edge detection can be also accomplished on one template by the proper choice of the strength and direction of the external magnetic field. It is important to note that none of the ME cells in the network has an individual contact, or a bias wire. The addressing of an individual cell is via the interference of two spin waves generated by the micro strips located at the edges of the structure as illustrated in Figure 14(a). The later offers an original solution to the interconnect problem inherent to the most of the proposed nano-CNNs. Instead of a large number of wires or a crossbar structure, nano-cells can be addressed via wave interference produced by just two micro antennas. Another potential advantage of using spin waves is the possibility to increase the radius of interaction R between the cells within CNN. In contrast to the other proposals exploiting only local interaction between the nearest neighbor cells, a relatively long coherence length allows to connect a large number of cells at a time. Though magnonic CNN has many appealing properties, the integration of ME cells with spin wave buses remains the main challenge. More practically feasible are the analog logic devices such as magnonic holographic memory, which operation entirely relies on the spin wave interference.
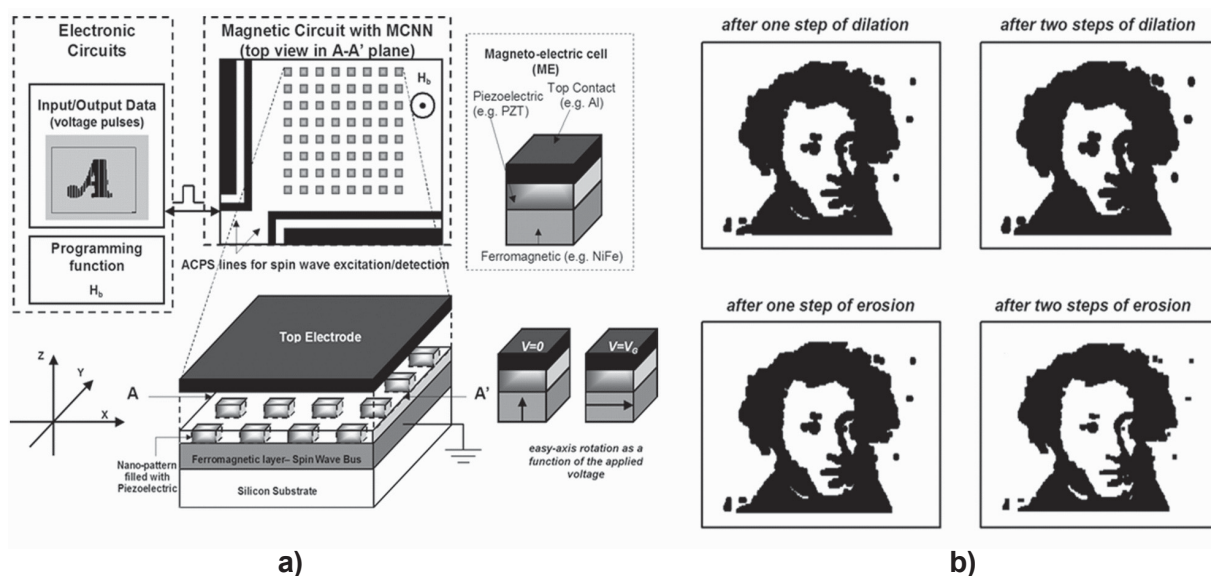

a)   b)

Fig. 14. (a) Schematic view of Magnonic Cellular Nonlinear Network (MCNN). There is an array of ME cells on the common ferromagnetic film-spin wave bus. Each cell is a bi-stable magnetic element. The interaction between the cells is via spin waves propagating though the spin wave bus. The read-in and read-out operations are accomplished by the edge micro antennas. (b) Results of numerical modeling illustrating image processing with MCNN. The black and the white pixels correspond to the two magnetic states of the ME cells (2008)

Holographic techniques have been extensively developed in optics and the unique capabilities of holographic approach for data storage and processing have been well-described in a number of works [72, 73]. The concept of holography is based on the use of wave interference and diffraction, which can be also implemented in spin wave devices [61]. The concept of Magnonic Holographic Memory (MHM) for data storage and data processing has been recently proposed [74]. MHM evolves the general idea of optical approach to applications in the magnetic domain aimed to combine the advantages of magnetic data storage with the unique capabilities for read-in and read-out provided by spin waves. At the same time, the use of spin waves implies certain requirements on the memory design, which are mainly associated with the need to preserve the energy of the spin wave carrying signals and the mechanisms of spin wave excitation and detection. The schematics of MHM as described in Ref. [74] are shown in Figure 15(a). It comprises two major

components: a magnetic matrix and an array of spin wave generating/detecting elements – input/output ports. Spin waves are excited by the elements on one or several sides of the matrix, propagate through the matrix and detected on the other side of the structure. For simplicity, the matrix is depicted as a two-dimensional grid of magnetic wires. These wires serve as a media for spin wave propagation – spin wave buses. The elementary mesh of the grid is a cross-junction between the two orthogonal magnetic wires as shown in Figure 15(a). There is a nano-magnet on the top of each junction. Each of these nano-magnets is a memory element holding information encoded in the magnetization state. The nano-magnet can be designed to have two or several thermally stable states for magnetization, where the number of states defines the number of logic bits stored in each junction. The spins of the nano-magnet are coupled to the spins of the junction magnetic wires via the exchange and/or dipole-dipole coupling affecting the phase of the propagation of
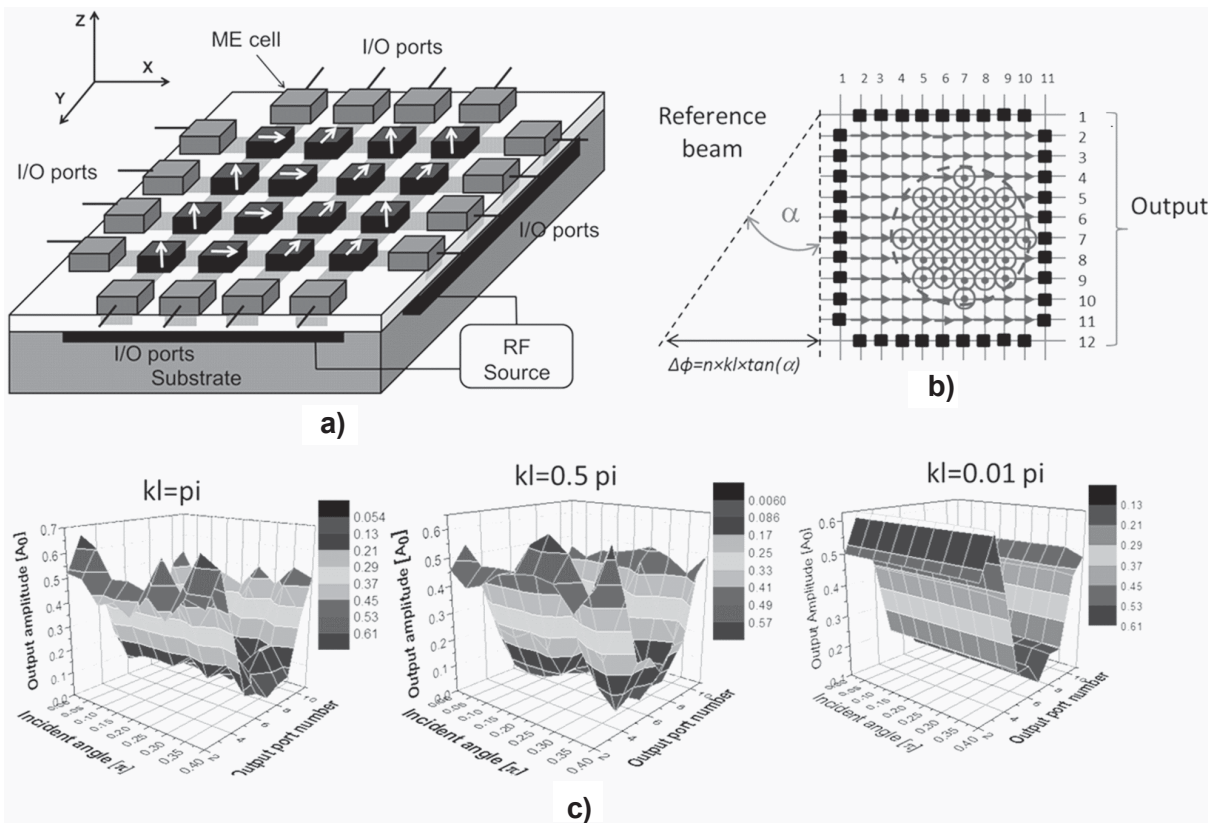

Fig. 15. (a) The schematics of the Magnonic Holographic Memory. I/O ports at the edges of the device are ME cells aimed to convert input electric signals into spin waves and, vice versa. The core of the structure is a two-dimensional grid of fer-romagnetic waveguides connected via magnetic cross junctions aimed to transmit spin waves between the input and output ports. (b) The input beam is generated by the ME cells on the left side of the structure, and the output is detected by the ME cells on the right side. The angle of illumination is controlled by the phase shift of the spin wave emitting cells. (c) The maps showing the output form the same template as a function of the incident angle. The simulations were carried out for three wavenumbers k: kl=π, kl=0.5π , kl=0.01π (2013)

spin waves. The phase change received by the spin wave depends on the strength and the direction of the magnetic field produced by the nano-magnet. At the same time, the spins of nano-magnet are affected by the local magnetization change caused by the propagating spin waves. We consider two modes of operations: read-in and read-out. In the read-in mode, the magnetic state of the junction can be switched if the amplitude of the transmitted spin wave exceeds some threshold value. In the read-out mode, the amplitudes of the propagating spin waves are too small to overcome the energy barrier between the states. So, the magnetization of the junction remains constant in the read-out mode.

The input spin wave beam is generated by the ME cells on the left side of the structure, and the output is detected by the ME cells on the right side. The angle of the incident beam α is controlled by the we introduced a phase shift among the spin wave emitting cells $\Delta\varphi=j\cdot kl\cdot tan(\alpha)$. The maps in Figure 15(c) show the output detected by the ME cells on the right side as a function of the incident angle. The simulations were carried out for three wavenumbers k: $kl=\pi$, $kl=0.5\pi$, $kl=0.01\pi$. As one can see from Figure 15(c), the output does vary as a function of the incident angle. The angle dependence of the output disappear in the long wavelength limit $kl=0.01\pi$, where the wavelength of the illuminating beam is much longer than the size of the junction. These results demonstrate the capabilities of magnonic hologram for recording multiple images in the same structure. According to the estimates [60], magnonic holographic devices can provide up 1Tb/cm^2 data storage density and provide data processing rate exceeding 10^{18} bits/s/cm^2.

Recently, a first 2-bit magnonic holographic memory has been experimentally demonstrated [75]. The magnetic matrix is a double-cross structure made of yttrium iron garnet $Y_3Fe_2(FeO_4)_3$ (YIG) epitaxially grown on gadolinium gallium garnet $Gd_3Ga_5O_{12}$ substrate with (111) crystallographic orientation. YIG film has ferromagnetic resonance (FMR) linewidth $2\Delta H\approx0.5Oe$, saturation magnetization $4\pi M_s=1750G$, and thickness d=3.6μm. This material is chosen due to its long spin wave coherence length and relatively low damping [76], which makes it the best candidate for room temperature spin wave devices prototyping. The length of the whole structure is 3mm, the width of the arm in 360μm. There are two micro-magnets on the top of the cross junctions. These magnets are the memory elements, where logic bits are encoded into the two possible directions for magnetization. There are six

micro-antennas fabricated on the top of the YIG waveguides. These antennas are used to excite spin wave in YIG material and to detect the inductive voltage produced by the propagating spin waves. Figure 16 shows the set of three holograms obtained for the three configurations of the top micro-magnets as illustrated by the schematics: A) two micro-magnets aligned in the same direction perpendicular to the long axis; B) the magnets are directed in the orthogonal directions; and C) both magnets are directed along the long axis. The red markers show the experimentally measured data (inductive voltage in millivolts) obtained at different phases of the four generated spin waves. The cyan surface is a computer reconstructed 3-D plot. The excitation frequency is 5.40 GHz, the bias magnetic field is 1000 Oe. All experiments are done at room temperature. As one can see from Figure 16, the state of the micro-magnet significantly changes the output. The three holograms clearly demonstrate the unique signature defined by the magnetic state of the micro-magnet. The internal state of the holographic memory can be reconstructed by the difference in amplitude as well as the phase-dependent distribution of the output. These experimental results show the feasibility of applying the holographic techniques in magnetic structures, combining the advantages of magnetic data storage with the wave-based information transfer. Though spin waves cannot compete with photons in terms of the propagation speed and exhibit much higher losses, magnonic holographic devices may be more suitable for nanometer scale integration with electronic circuits.

4. Discussion and Summary

Magnonic logic devices possess its unique advantages and shortcomings. On one hand, the utilization of the spin waves of submicron wavelength provides an intrigue opportunity to realize a wave-like computer (similar to the optical computer) at the nanometer scale. Spin waves can be efficiently directed by magnetic waveguides and modulated by the applied magnetic field or by electric field via the magnetoelectric effect described above. With the latter, it is possible to directly convert from a voltage to spin waves and vice versa, which makes spin wave-based circuits compatible with conventional electron-based devices. On the other hand, there are some fundamental drawbacks inherent to spin waves, which will limit the performance of the spin wave-based devices. These disadvantages are (i) relatively low group velocity (10^7cm/s), and (ii) short decay time for propagating spin wave at
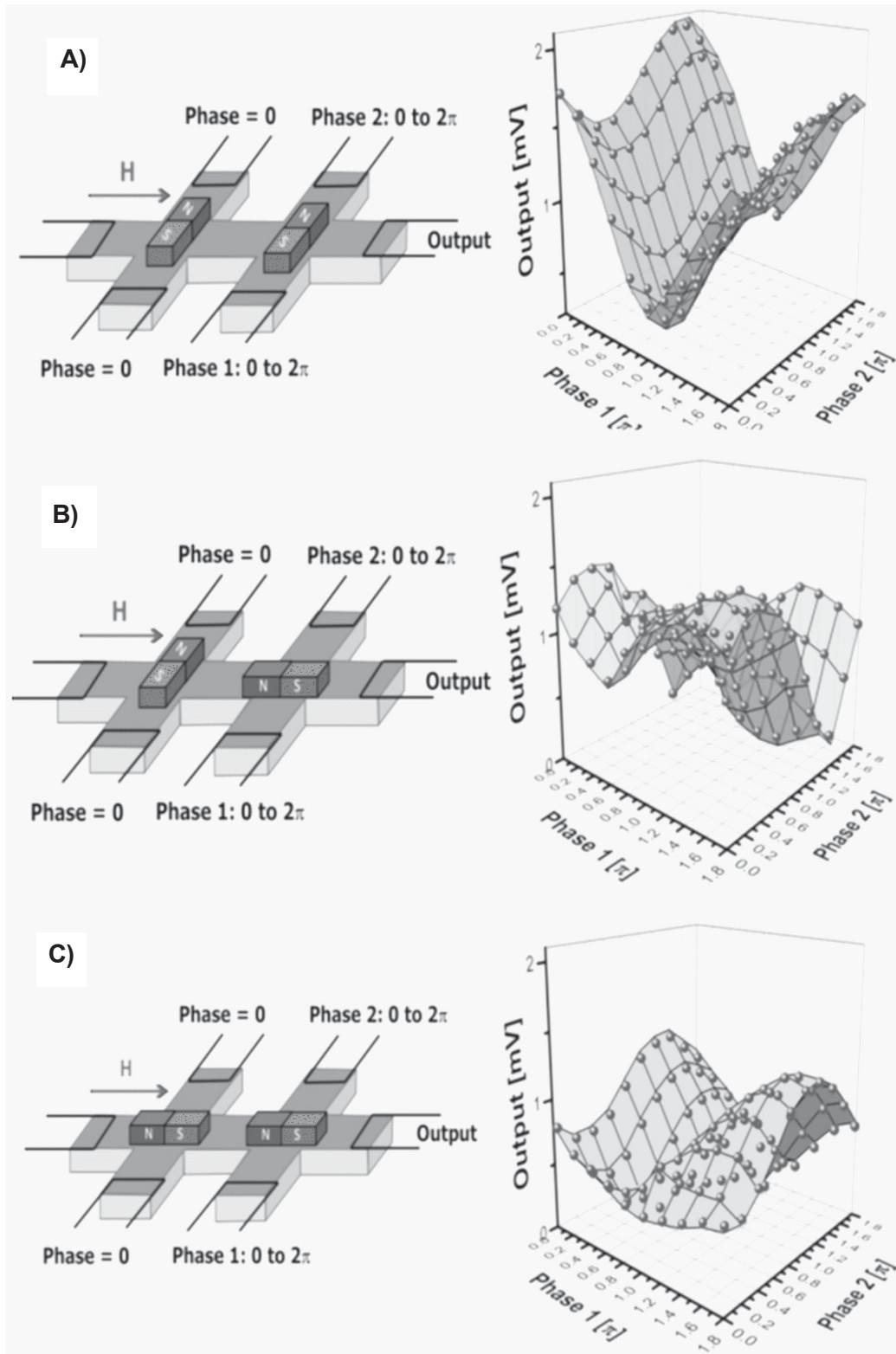
Fig.16. A set of three holograms obtained for the three configurations of the top micro-magnets as illustrated by the schematics on the top: A) two micro-magnets aligned in the same direction perpendicular to the long axis; B) the magnets are directed in the orthogonal directions; and C) both magnets are directed along the long axis. The red markers show the experimentally measured data (inductive voltage in millivolts) obtained at different phases of the four generated spin waves. The cyan surface is a computer reconstructed 3-D plot. The excitation frequency is 5.4GHz, the bias magnetic field is 1000 Oe, All experiments are done at room temperature

room temperature. Spin wave dispersion depends on the waveguide geometry, the strength of the bias magnetic field, and varies for different spin wave modes. In the best scenario, spin wave signal is three orders of magnitude slower than the photons in silica or electromagnetic wave in a copper coaxial cable. The use of spin waves for information transmission implies a signal delay, which is l/v_g, where l is the propagation distance. The disadvantage associated with low group velocity is partially compensated by short (submicrons) propagation distances, resulting in 0.1-1.0ns time delay per each logic gate.

Another important disadvantage is associated with the spin wave signal damping during the propagation in the spin wave bus. The damping is caused by magnon-magnon, magnon-phonon scattering as well as the effect of the Eddy current in conducting magnetic materials. For example, the spin wave damping time in 100nm thick NiFe film is about 0.8ns at room temperature [4]. It means that a significant portion of the spin wave energy will be dissipated in the waveguide structure. Thus, spin wave buses cannot be considered as an alternative to metal conductors for electric signal transmission [77].

However, the construction of some logic gates with spin wave buses can be done with a fewer number of devices than required for the equivalent CMOS-based circuit. This is a fundamental advantage of using phases in addition to amplitude for information transmission and processing. Majority gate is an example of efficient construction of logic gate illustrating this advantage. Encoding a bit of information into the phase of the spin wave signal, affords the exploitation of spin wave superposition for Majority gate construction as described previously in the text. A large number of waveguides can be combined with *a single* magnetoelectric cell leading to the Majority gate operation. The whole gate can be scaled down to a single ferromagnetic wire with multiple magnetoelectic cells. In contrast, the number of CMOSs required for Majority gate scales proportional to the number of inputs. Majority logic is a way of implementing digital operations in a manner different from that of Boolean logic. In general, Majority logic is more powerful for implementing a given digital function with a smaller number of logic gates than CMOS [78]. For example, the full adder may be constructed with three majority gates and two inverters (3 magnetoelectric cells and 2 modulators). In contrast, a Boolean-based implementation requires a larger circuit with seven or eight gate elements (about 25–30 MOSFETs)

[79]. The main reason Majority logic has been out of stage for decades is because its CMOS realization is inefficient. Only with the development of novel devices such as Josephson junction circuits, which is not feasible at room temperature [80], and quantum cellular automata [81], the Majority logic gates become efficient for practical implementation. It is also feasible to make a reconfigurable Majority gates whose logic operation can be controlled by the spin wave phase modulators. In turn, the integration of reconfigurable Majority gates provides a route to building both general purpose and special task architectures such as Cellular Automata, Field Programmable Gate Arrays and others.

An important question to ask is whether or not spin-wave based logic circuit can have lower power dissipation than those in the same function CMOS-based circuit? The energy per operation in the magnonic logic circuits is mainly defined by the energy required for spin wave excitation. We want to emphasize the difference between the volatile and non-volatile magnonic circuits in terms of power consumption. In the most volatile spin wave logic circuits described in this Chapter, these are the only power consuming elements (e.g. magnonic holographic memory). The operation of non-volatile logic circuits (e.g. as shown in Figure 6) requires an additional energy for magnetization switching in the output memory elements. Synthetic multiferroic elements (ME cells) are the most promising elements from the power consumption point of view. According to the experimental data [82], the electric field required for magnetization rotation on 90 degrees in Ni/PZT synthetic multiferroic is about 1.2MV/m. The latter promises a very low, order of atto Joule, energy per switch achievable in nanometer scale ME cells (e.g. 24aJ for 100nm×100nm ME cell with 0.8μm PZT) [53]. Thus, the maximum power dissipation density per $1\mu m^2$ area circuit operating at 1GHz frequency can be estimated as $7.2W/cm^2$. In the multi-frequency circuits, an addition of an extra operating frequency would linearly increase the power dissipation in the circuit [54].

The comparison between the magnonic and CMOS-based logic devices should be done at the circuit level by comparing the overall circuit parameters such the number of functions per area per time, time delay per operation, and energy required for logic function. In Table, we summarized the estimates for magnonic Full Adder circuit and compare them with the parameters of the CMOS-based circuit. The data for the Full Adder circuit made on 45nm and 32nm CMOS technology is based on the

ITRS projections [83] and available data on current technology [84]. The data for the magnonic circuits is based on the design described in [53] and the above made estimates. Magnonic circuit predicts significant ~100X advantage in minimizing circuit area due to the fewer number of elements required per circuit (e.g. 5 ME cells versus 25–30 CMOSs). At the same time, magnonic logic circuits would be slower than the CMOS counterparts. In Table, we have shown two numbers for time delay corresponding to volatile and non-volatile circuits. The delay time of the volatile circuit is mainly defined by the spin wave group velocity, while the delay time of the non-volatile circuit is restricted by the relaxation time of the output ME cell. The most prominent ~ 1000X advantage over CMOS circuitry is expected in minimizing power consumption. Besides the great reduction of active power, there is no static power consumption in magnonic logic circuits based on non-volatile magnetic cells. The overall functional throughput is about 100 times higher for magnonic logic circuits due to the smaller circuit area.

Comparison between the spin wave-based and the conventional Full Adder circuits

Parameters	45nm CMOS	32nm CMOS	$\lambda = 45$nm	$\lambda = 32$nm
Area	6.4 μm^2	3.2 μm^2	0.05 μm^2	0.026 μm^2
Time Delay	12 ps	10 ps	13.5 ps /0.1 ns	9.6 ps/0.1 ns
Functional	1.3×10^9	3.1×10^9	1.48×10^{11}	4.0×10^{11}
Throughput	Ops/[ns cm^2]	Ops/[ns cm^2]	Ops/[ns cm^2]	Ops/[ns cm^2]
Energy per Operation	12fJ	10fJ	24aJ	15aJ
Static Power	> 70nW	> 70nW	–	–

In **Conclusion**, magnonic logic devices are among the most promising alternative approaches to post-"beyond CMOS" logic circuitry by offering a significant functional throughput enhancement. The reason for this enhancement is the use of phase in addition to amplitude for achieving logic functionality. Coding information into the phase of the propagating spin waves makes it possible to utilize the waveguides as passive logic elements and reduce the number of elements per circuit. The ability to use multiple frequencies as independent information channels opens a new dimension for functional throughput enhancement as well. There are many questions to be answered and many technological issues to be resolved before magnonic logic circuits will find any practical application. One of the main challenges is associated with the scaling down the operational wavelength to sub-micrometer range. As for today, all of the demonstrated prototypes utilize the spin waves of micrometer scale wavelength, which makes them immune with respect to the waveguide structure variations. It is not clear if the scaling to the deep sub-micrometer range would significantly affect the signal to noise ratio as well as the speed of propagation. In spite of the number of technical issues, magnonic logic devices offer a new route to functional throughput enhancement with a substation performance pay off. Most probably, magnonic logic devices such as magnonic holographic memory will not replace but complement the existing logic circuitry in special task data processing.

References

1. International Technology Roadmap for Semiconductors. *Semiconductor Industry Association,* 2005. Available at: http://www.semiconductors.org/main/2005_international_technology_roadmap_for_semiconductors_itrs/ (accessed 08 September 2017).

2. Schilz W. Spin-wave propagation in epitaxial YIG films. *Philips Research Reports,* 1973, vol. 28, pp. 50–65.

3. Silva T. J., Lee C. S., Crawford T. M., Rogers C. T. Inductive measurement of ultrafast magnetization dynamics in thin-film Permalloy. *Journal of Applied Physics,* 1999, vol. 85, pp. 7849–7862. DOI: http://dx.doi.org/10.1063/1.370596.

4. Covington M., Crawford T. M., Parker G. J. Time-resolved measurement of propagating spin waves in ferromagnetic thin films. *Physical Review Letters,* 2002, vol. 89, no. 237202.

5. Bailleul M., Ollig D., Fermon C., Demokritov S. Spin waves propagation and confinement in conducting films at the micrometer scale. *Europhysics Letters,* 2001, vol. 56, pp. 741–747.

6. Nikitov S. A., Kalyabin D. V., Lisenkov I. V., Slavin A., Barabanenkov Yu. N., Osokin S. A., Sadovnikov A. V., Beginin E. N., Morozova M. A., Sharaevsky Yu. P., Filimonov Yu. A., Khivintsev Yu. V., Vysotsky S. L., Sakharov V. K., Pavlov E. S. Magnonics: a new research area in spintronics and spin wave electronics.

Phys. Usp., 2015, vol. 58, p. 1099. DOI:10.3367/UFNe.0185.201510m.1099.

7. Khitun A., Wang K. L. Nano scale computational architectures with Spin Wave Bus. *Superlattices and Microstructures,* 2005, vol. 38, no. 9, pp. 184–200.

8. Eshaghian-Wilner M. M., Khitun A., Navab S., Wang K. A nano-scale reconfigurable mesh with spin waves. *CF 06 Proceedings of the 3rd conference on Computing frontiers,* New York, NY, USA, 2006, pp. 65–70.

9. Khitun A., Wang K. L. Nano logic circuits with spin wave bus. *Journal of Nanoelectronics and Optoelectronics*, 2006, vol. 1, pp.71–73.

10. Wang K. L., Khitun A., Flood A. H. Interconnects for nanoelectronics. *Proceedings of the IEEE 2005 International Interconnect Technology Conference* (IEEE Cat. No. 05TH8780), 2005, pp. 231–233.

11. Wang K. L., Khitun A., Flood A. H. Interconnects for nanoelectronics. *IEEE Xplore digital laboratory*, 2005 (INSPEC Accession Number: 8531782). DOI: 10.1109/IITC.2005.1499994.

12. Kozhanov A., Ouellette D., Rodwell M., Allen S. J., Jacob A. P., Lee D. W., Wang S. X. Dispersion and spin wave "tunneling" in nanostructured magnetostatic spin waveguides. *Journal of Applied Physics,* 2009, Apr. 1, vol. 105, no. 7, p. 311.

13. Kozhanov A., Ouellette D., Rodwell M., Allen S. J., Lee D. W., Wang S. X. Micro-structured ferromagnetic tubes for spin wave excitation. *Journal of Applied Physics,* 2011, Apr. 1, vol. 109, no. 7, p. 333.

14. Khitun A., Bao M., Wang K. L. Spin Wave Magnetic NanoFabric: A New Approach to Spin-based Logic Circuitry. *IEEE Transactions on Magnetics,* 2008, vol. 44, pp. 2141–2153.

15. Kaka S., Pufall M. R., Rippard W. H., Silva T. J., Russek S. E., Katine J. A. Mutual phase-locking of microwave spin torque nano-oscillators. *Nature,* 2005, Sep. 15, vol. 437(7057), pp. 389–392.

16. Cherepov S., Khalili-Amiri P., Alzate J. G., Wong K., Lewis M., Upadhyaya P., Nath J., Bao M., Bur A., Wu T., Carman G. P., Khitun A., Wang K. L. Electric-field-induced spin wave generation using multiferroic magnetoelectric cells. *Applied Physics Letters*, Feb. 2014, vol. 104, no. 8, p. 082403.

17. Kozhanov A., Ouellette D., Rodwell M., Lee D. W., Wang S. X., Allen S. J. Magnetostatic Spin-Wave Modes in Ferromagnetic Tube. *IEEE Transactions on Magnetics,* 2009, vol. 45, no. 10, pp. 4223–4225.

18. Berger L. Low-field magnetoresistance and domain drag in ferromagnets. *Journal of Applied Physics,* 1978, vol. 49, no. 3, p. 2156. DOI: http://dx.doi.org/10.1063/1.324716.

19. Slonczewski J. C. Current-driven excitation of magnetic multilayers. *Journal of Magnetism and Magnetic Materials,* 1996, vol. 159, no. 1–2, pp. L1–7.

20. Demidov V. E., Urazhdin S., Demokritov S. O. Direct observation and mapping of spin waves emitted by spin-torque nano-oscillators. *Nature Materials,* 2010, vol. 9, no. 12, pp. 984–988.

21. Tsoi M., Jansen A. G. M., Bass J., Chiang W. C., Tsoi V., Wyder P. Generation and detection of phase-coherent current-driven magnons in magnetic multilayers. *Nature,* 2000, vol. 406, pp. 46–48.

22. Eerenstein W., Mathur N. D., Scott J. F. Multiferroic and magnetoelectric materials. *Nature,* 2006, vol. 442, pp. 759–765.

23. Wang J., Neaton J. B., Zheng H., Nagarajan V., Ogale S. B., Liu B., Viehland D., Vaithyanathan V., Schlom D. G., Waghmare U. V., Spaldin N. A., Rabe K. M., Wuttig M., Ramesh R. Epitaxial BiFeO$_3$ multiferroic thin film heterostructures. *Science,* 2003, March 14, vol. 299, pp. 1719–1722.

24. Roy K., Bandyopadhyay S., Atulasimha J. Hybrid spintronics and straintronics: A magnetic technology for ultra low energy computing and signal processing. *Applied Physics Letters,* 2011, Aug 8, vol. 99, p. 063108.

25. Wu T., Bur A., Zhao P., Mohanchandra K. P., Wong K., Wang K. L., Lynch C. S., Carman G. P. Giant electric-field-induced reversible and permanent magnetization reorientation on magnetoelectric Ni/(011) [Pb(Mg1/3Nb2/3)O$_3$](1−x)–[PbTiO$_3$]x heterostructure. *Applied Physics Letters,* 2011, vol. 98, p. 012504–7.

26. Srinivasan G., Rasmussen E. T., Gallegos J., Srinivasan R., Bokhan Yu I., Laletin V. M. Magnetoelectric bilayer and multilayer structures of magnetostrictive and piezoelectric oxides. *Physical Review B (Condensed Matter and Materials Physics),* 2001, vol. 64, p. 2144081.

27. Van Den Boomgaard J., Terrell D. R., Born R. A. J., Giller H. An in situ grown eutectic magnetoelectric composite material. I. Composition and unidirectional solidification. *Journal of Materials Science,* 1974, vol. 9, pp. 1705–1709.

28. Jungho R., Carazo V., Uchino K., Hyoun-Ee K. Magnetoelectric properties in piezoelectric and magnetostrictive laminate composites. *Japanese Journal of Applied Physics, Part 1 (Regular Papers, Short Notes & Review Papers),* 2001, vol. 40, pp. 4948–4951.

29. Shabadi P., Khitun A., Narayanan P., Mingqiang B., Koren I., Wang K. L., Moritz C. A. Towards logic functions as the device. *2010 IEEE/ACM International Symposium on Nanoscale Architectures (NANOARCH 2010),* 2010, vol. 01, pp.11–16.

30. Cherepov S., Khalili Amiri P., Alzate J. G., Kin W., Lewis M., Upadhyaya P., Nath J., Mingqian B., Bur A., Tao W., Carman G. P., Khitun A., Wang K. L. Electric-field-induced spin wave generation using multiferroic magnetoelectric cells. *Applied Physics Letters,* 2014, Feb. 24, vol. 104, p. 082403.

31. Khitun A., Wang K. Nano scale computational architectures with Spin Wave Bus. *Superlattices & Microstructures,* 2005, vol. 38, pp. 184–200.

32. Kozhanov A., Ouellette D., Griffith Z., Rodwell M., Jacob A. P., Lee D. W., Wang S. X., Allen S. J. Dispersion in magnetostatic CoTaZr spin waveguides. *Applied Physics Letters,* 2009, Jan. 5, vol. 94, p. 012505.

33. Damon R. W., Eshbach J. Magnetostatic modes of a ferromagnet slab. *Journal of Physics and Chemistry of Solids,* 1961, vol. 19, pp. 308–320.

34. Khitun A., Nikonov D. E., Wang K. L. Magnetoelectric spin wave amplifier for spin wave logic circuits. *Journal of Applied Physics,* 2009, vol. 106, p. 123909.

35. Arias R., Mills D. Magnetostatic modes in ferromagnetic nanowires. *Physical Review B,* 2004, vol. 70, p. 094414.

36. Arias R., Mills D. Magnetostatic modes in ferromagnetic nanowires. II. A method for cross sections with very large aspect ratio. *Physical Review B,* 2005, vol. 72, p. 104418.

37. Adam J. D., Davis L. E., Dionne G. F., Schloemann E. F., Stitzer S. N. Ferrite devices and materials. *IEEE Transactions on Microwave Theory and Techniques,* 2002, vol. 50, pp. 721–737.

38. Kuanr B., Harward I. R., Marvin D. L., Fal T., Camley R. E., Mills D. L., Celinski Z. High-frequency signal processing using ferromagnetic metals. *IEEE Transactions on Magnetics,* 2005, vol. 41, pp. 3538–3543.

39. Almeida N., Mills D. Eddy currents and spin excitations in conducting ferromagnetic films. *Physical Review B,* 1996, vol. 53, p. 12232.

40. Demidov V., Jersch J., Demokritov S., Rott K., Krzysteczko P., Reiss G. Transformation of propagating spin-wave modes in microscopic waveguides with variable width. *Physical Review B,* 2009, vol. 79, p. 054417.

41. Vogt K., Schultheiss H., Jain S., Pearson J., Hoffmann A., Bader S., Hillebrands B. Spin waves turning a corner. *Applied Physics Letters,* 2012, vol. 101, p. 042410.

42. Birt D. R., O'Gorman B., Tsoi M., Li X., Demidov V. E., Demokritov S. O. Diffraction of spin waves from a submicrometer-size defect in a microwaveguide. *Applied Physics Letters,* 2009, vol. 95, p. 122510.

43. Kozhanov A., Ouellette D., Rodwell M., Allen S., Jacob A., Lee D., Wang S. Dispersion and spin wave "tunneling" in nanostructured magnetostatic spin waveguides. *Journal of Applied Physics,* 2009, vol. 105, p. 07D311.

44. Schneider T., Serga A., Chumak A., Hillebrands B., Stamps R., Kostylev M. Spin-wave tunnelling through a mechanical gap. *EPL (Europhysics Letters),* 2010, vol. 90, p. 27003.

45. Kozhanov A., Anferov A., Jacob A. P., Allen S. J. Spin Wave Scattering in Ferromagnetic Cross., 2012, *arXiv preprint arXiv:1211.1259.*

46. Barman A., Kruglyak V., Hicken R., Rowe J., Kundrotaite A., Scott J., Rahman M. Imaging the dephasing of spin wave modes in a square thin film magnetic element. *Physical Review B,* 2004, vol. 69, p. 174426.

47. Demokritov S., Serga A., Andre A., Demidov V., Kostylev M., Hillebrands B., Slavin A. Tunneling of dipolar spin waves through a region of inhomogeneous magnetic field. *Physical Review Letters,* 2004, vol. 93, p. 047201.

48. Hansen U.-H., Gatzen M., Demidov V. E., Demokritov S. O. Resonant tunneling of spin-wave packets via quantized states in potential wells. *Physical Review Letters,* 2007, vol. 99, p. 127204.

49. Kruglyak V., Demokritov S., Grundler D. Magnonics. *Journal of Physics D: Applied Physics,* 2010, vol. 43, p. 264001.

50. Kostylev M. P., Serga A. A., Schneider T., Leven B., Hillebrands B. Spin-wave logical gates. *Applied Physics Letters,* 2005, vol. 87, p. 153501.

51. Schneider T., Serga A. A., Leven B., Hillebrands B., Stamps R. L., Kostylev M. P. Realization of spin-wave logic gates. *Applied Physics Letters,* 2008, vol. 92, p. 022505.

52. Lee K.-S., Kim S.-K. Conceptual design of spin wave logic gates based on a Mach-Zehnder-type spin wave interferometer for universal logic functions. *Journal of Applied Physics,* 2008, vol. 104, p. 053909.

53. Khitun A., Wang K. L. Non-Volatile Magnonic Logic Circuits Engineering. *Journal of Applied Physics,* 2011, vol. 110, p. 034306.

54. Khitun A. Multi-frequency magnonic logic circuits for parallel data processing. *Journal of Applied Physics,* 2012, March 1, vol. 111, p. 054307.

55. Krivorotov I. Spin Torque Oscillator Majority Logic. *Western Institute of Nanoelectronics, Annual Review,* 2012, vol. Abstract 3.1, pp. 3–7.

56. Shabadi P., Khitun A., Narayanan P., Bao M., Koren I., Wang K. L., Moritz C. A. Towards Logic Functions as the Device. *2010 IEEE/ACM International Symposium on Nanoscale Architectures (NANOARCH 2010),* 2010, vol. 01, pp.11–16.

57. Khitun A., Nikonov D. E., Wang K. L. Magnetoelectric spin wave amplifier for spin wave logic circuits. *J. Appl. Phys.,* 2009, vol. 106, p. 123909.

58. Nanayakkara A. A. K., Allen S. J., Jacob A. P., Kozhanov A. Cross junction spin wave logic architecture. *IEEE Transactions on Magnetics,* 2014, vol. 50, no. 3402204. DOI: 10.1109/TMAG.2014.2320632.

59. Khitun A., Bao M., Lee J.-Y., Wang K. L., Lee D. W., Wang S. X., Roshchin I. V. Inductively Coupled Circuits with Spin Wave Bus for Information Processing. *Journal of Nanoelectronics and Optoelectronics,* 2008, vol. 3, pp. 24–34.

60. Shabadi P., Khitun A., Wong K., Amiri P. K., Wang K. L., Andras C. A. Spin wave functions nanofabric update. *2011 IEEE/ACM International Symposium on Nanoscale Architectures (NANOARCH 2011),* 2011, vol. 01, pp. 107–113.

61. Khitun A. Magnonic Holographic Devices for Special Type Data Processing. *Journal of Applied Physics,* 2013, vol. 113, p. 164503.

62. Lee S. H. *Optical Information Processing Fundamentals.* Berlin, Germany: Springer, 1981. 237 p.

63. International Technology Roadmap for Semiconductors. *Semiconductor Industry Association,* 2011. Available at: http://www.semiconductors.org/main/2011_international_technology_road map_for_semiconductors_itrs (accessed 08 September 2017).

64. Krawczyk M., Puszkarski H. Magnonic crystal theory of the spin wave frequency gap in low-dopoed manganites.

Journal of Applied Physics, 2006, vol. 100, p. 073905.

65. Chua L. O., Yang L. Cellular neural networks: theory. *IEEE Transactions on Circuits & Systems,* 1988, vol. 35, pp. 1257–1272.

66. Ambs P. Optical Computing: A 60-Year Adventure. *Advances in Optical Technologies Volume (2010),* 2010, vol. 2010, pp. 372652.

67. Matsumoto T., Chua L. O., Yokohama T. Image thinning with a cellular neural network. *IEEE Transactions on Circuits & Systems,* 1990, vol. 37, pp. 638–640.

68. Krieg K. R., Chua L. O., Yang L. Analog signal processing using cellular neural networks. *IEEE International Symposium on Circuits and Systems* (Cat. no. 90CH2868-8). New York, NY, USA, 1990, vol. 2, pp. 958–961.

69. Roska T., Boros T., Thiran P., Chua L. O. Detecting simple motion using cellular neural networks. *1990 IEEE International Workshop on Cellular Neural Networks and their Applications, CNNA-90* (Cat. no. 90TH0312-9). *IEEE.* New York, NY, USA, 1990, pp. 127–138.

70. Venetianer P. L., Werblin F., Roska T., Chua L. O. Analogic CNN algorithms for some image compression and restoration tasks. *IEEE Transactions on Circuits & Systems I-Fundamental Theory & Applications,* 1995, vol. 42, pp. 278–284.

71. Khitun A., Mingqiang B., Wang K. L. Magnetic Cellular Nonlinear Network with Spin Wave Bus. *12th International Workshop on Cellular Nanoscale Networks and their Applications (CNNA 2010),* 2010, no. 11207525. DOI: 10.1109/CNNA.2010.5430306.

72. Gabor D. A new microscopic principle. *Nature,* 1948, vol. 161, pp. 777–778.

73. Hariharan P. *Optical Holography: Principles, Techniques and Applications.* Cambridge University Press, 1996. 406 p.

74. Khitun A. Magnonic holographic devices for special type

75. Gertz F., Kozhanov A., Filimonov Y., Khitun A. Magnonic Holographic Memory. *Magnetics, IEEE Transactions on,* 2015, May 15, vol. 51, pp. 4002905–4002910.

76. Serga A. A., Chumak A. V., Hillebrands B. YIG MAgnonics. *Journal of Physics D: Applied Physics,* 2010, vol. 43, p. 264002.

77. Khitun A., Nikonov D. E., Bao M., Galatsis K., Wang K. L. Feasibility Study of Logic Circuits with Spin Wave Bus. Nanotechnology, 2007, vol. 18, iss. 46, p. 465202. DOI: 10.1088/0957-4484/18/46/465202.

78. Meo A. R. Majority Gate Networks. *IEEE Transactions on Electronic Computers,* 1966, vol. EC-15, pp. 606–618.

79. Oya T., Asai T., Fukui T., Amemiya Y. A majority-logic device using an irreversible single-electron box. *IEEE Transactions on Nanotechnology,* 2003, vol. 2, pp. 15–22.

80. Loe K. F., Goto E. Analysis of flux input and output Josephson pair device. in *IEEE Transactions on Magnetics,* March 1985, vol. MAG-21, no. 2, pp. 884–887.

81. Lent C. S., Tougaw P. D., Porod W., Bernstein G. H. Quantum cellular automata. *Nanotechnology,* 1993, vol. 4, pp. 49–57.

82. Chung T. K., Keller S., Carman G. P. Electric-field-induced Reversible Magnetic Single-domain Evolution in a Magnetoelectric Thin Film. *Applied Physics Letters,* 2009, vol. 94, no. 13, p. 132501. DOI: http://dx.doi.org/10.1063/1.3110047.

83. International Technology Roadmap for Semiconductors. *Semiconductor Industry Association,* 2007. Available at: https://www.semiconductors.org/main/2007_international_technology_roadmap_for_semiconductors_itrs/ (accessed 08 September 2017).

84. Tsu-Jae King Liu, Kelin Kuhn. *CMOS and Beyond. Logic Switches for Terascale Integrated Circuits.* Cambridge University Press, 2015. 436 p.